Journal of Statistical Physics, Vol. 102, Nos. 1/2, 2001

Fixed-Boundary Octagonal Random Tilings: A Combinatorial Approach

N. Destainville,[1] R. Mosseri,[2] and F. Bailly[3]

Received March 6, 2000

Some combinatorial properties of fixed boundary rhombus random tilings with octagonal symmetry are studied. A geometrical analysis of their configuration space is given as well as a description in terms of discrete dynamical systems, thus generalizing previous results on the more restricted class of codimension-one tilings. In particular this method gives access to counting formulas, which are directly related to questions of entropy in these statistical systems. Methods and tools from the field of enumerative combinatorics are used.

KEY WORDS: Random tilings; generalized partitions; configurational entropy; discrete dynamical systems; Young tableaux.

INTRODUCTION

The experimental discovery of quasicrystalline alloys[(1)] led to extensive work on space tilings over the last 15 years, as it became clear that quasi-periodic, and not only periodic, structures could play important role in solid state physics. Indeed, the atomic structure of the highest quality quasicrystals has been found to follow closely the 3-dimensional icosahedral analogues of the celebrated pentagonal Penrose tilings.[(2)] Among the many questions that are still open in this field, the origin of their stability is one of the mostly highly debated. Physical explanations range from an electronic stabilization mechanism (refinements on the old

[1] Laboratoire de Physique Quantique—IRSAMC—UMR 5626, Université Paul Sabatier, 118, route de Narbonne, 31062 Toulouse Cedex 04, France.
[2] Groupe de Physique du Solide, Tour 23, 5ième étage, Universités Paris 7 et 6, 2, place Jussieu, 75251 Paris Cedex 05, France.
[3] Laboratoire de Physique du Solide—CNRS, 1, place Aristide Briand, 92195 Meudon Cedex, France.

0022-4715/01/0100-0147$19.50/0

Hume–Rothery approach) to an original entropic stabilization, allowed by specific phason modes which can be generated in quasiperiodic tilings. Our purpose here is not to discuss the relative merits of the different mechanisms, but to analyze in detail the combinatorial problems associated with configurational entropy in random tilings.

This paper follows a previous one[3] in which the general framework was introduced, as well as specific results concerning codimension-one tilings. The d-dimensional random tilings of interest are made of rhombi ($d=2$) or rhombohedra ($d=3$), or even higher dimensional analogues. These tilings are projections onto a d-dimensional Euclidean space of a d-dimensional faceted membrane cut into a D-dimensional hypercubic lattice ($D>d$). The "codimension" of a tiling is the difference $D-d$, and the tiling is said to be of type $D\to d$. In ref. 3, we discussed the codimension-one case for tilings with specific (fixed) boundary conditions. This allows us to write a one-to-one correspondence between tilings and combinatorial objects, called partitions. We built a geometrical description of the partition configuration space in terms of integral points in a high dimensional space, the entropy being computed from the integral volume of a specific convex polytope in that space. The occurrence of multiplicative and additive formulas for this volume was analyzed in detail, and given a simple geometrical meaning in the latter case in terms of a simplicial decomposition of the convex polytope.

The aim of the present paper is the analysis of random tilings of higher codimension, starting with the simplest $4\to 2$ case. Studying these cases is of direct importance in the context of quasicrystal physics, since all the quasiperiodic tilings encountered in this field are of codimension greater than one ($5\to 2$ for the pentagonal Penrose tiling, and $6\to 3$ in the icosahedral case). Tilings of type $4\to 2$ correspond to the so-called octagonal family, which was also observed in concrete alloys.[4] Although they are the simplest, "octagonal" random tilings already present most of the difficulties which, up to now, have forbidden the derivation of exact results for the large class of random tilings derived from hypercubic tilings.[5] Note that exact results exist (for the entropy) for other kinds of tilings, such as the square–triangle tiling,[6,7] rectangle–triangle tilings,[8,9] or large codimension tilings.[10] Note however that the present point of view does not apply to the two first examples since there exist no partition representation for such tilings.

Our analysis for the $4\to 2$ tilings follow from a generalization of the simple partition problem, valid in case of codimension one, to an iterated partition problem, which was proposed earlier,[11] and has already led to some preliminary numerical results. Here we describe the intricacy of the configuration space, which is no longer convex "as a whole," but remains

convex by parts. We show that despite its complexity, some exact but partial enumerative results can be obtained, although we must stress that the ultimate goal—an exact formula for the entropy—was not obtained and seems out of reach for the moment. We nevertheless believe that the present analysis is an important step in at least two directions: we give a very precise description of the configuration space and its simplex decomposition and we point out several very closely related problems in combinatorics, like the enumeration of sorting algorithms (Appendix B).

The paper is organized as follows. Section 1 recalls some older results and definitions, in particular the concept of de Bruijn lines and faceted membranes, and the bijection between standard partitions and codimension-one tilings. Section 2 focuses on higher codimension tilings, by introducing "generalized" partitions, and describing the particular structure that is inherited by the configuration space. Its properties in terms of local rearrangements of tiles (flips) are analyzed in detail. In Section 3, we discuss the decomposition of the configuration space into normal simplices, and we show the latter can be characterized thanks to a "descent theorem." This allows us to compute new enumerative formulas which were inaccessible by "brute-force" methods; these formulas are displayed in Section 4.

Even though this paper focuses on two-dimensional tilings and more precisely on octagonal ones, some results can easily be generalized to higher dimensional systems. The state of the art in the $D \to d$ cases is briefly discussed in Appendix D.

1. DEFINITIONS AND KNOWN RESULTS

In this paper we consider 2-dimensional tilings of rhombic tiles which fill a region of the Euclidean space without gaps or overlaps. The standard method for generating such structures consists of a selection of sites and tiles in a 4-dimensional lattice according to certain rules, followed by a projection onto the 2-dimensional subspace along a generic direction. We then say that we have a $4 \to 2$ tiling problem, or an octagonal one, in reference to the sub-class of ideal quasiperiodic Ammann tilings which have octagonal symmetry. The above procedure is also known as the "cut-and-project" method.[12–14] By construction, the so-obtained rhombic tiles are the projections of the 2-dimensional facets of the 4-dimensional hypercubic lattice. There are 6 different species of tiles, two squares and four 45 degree rhombi. Figures 1 and 11 show examples. In the cut-and-project language the difference between the higher and the lower dimensions is called the tiling *codimension*. In this case it is equal to 2.

We first recall some definitions and results which will prove to be useful throughout this paper. These definitions are given in a slightly more

general context than the octagonal case. The higher dimension will be denoted by D and the lower one by d.

1.1. De Bruijn Grids and Directed Membranes

Firstly, it should be mentioned that there exist two related classes of objects which can be put in one-to-one correspondence with random tilings: *de Bruijn grids* on the one hand, and *directed membranes* on the other hand.

De Bruijn grids[15, 16] are dual representations of tilings which can be useful to state or prove some results concerning tilings. There are a great number of publications dealing with these grids in the scientific literature (for example, see refs. 17 and 18), therefore we shall not give a complete presentation of these objects. Instead we shall give them an intuitive definition in the case of two-dimensional tilings. De Bruijn grids are made up of lines, the so-called de Bruijn lines, which are also called "worms." These lines join together the middles of opposite edges of rhombic tiles. Since the tiles are rhombi, it is always possible to extend these lines through the tiling up to the boundary. Such lines are displayed in Fig. 1. Any tile is crossed by two lines. There is no triple intersection point (condition of *regularity*). On the other hand, there are lines which can never intersect, even in an infinite tiling. They join rhombus edges of the same orientation, as illustrated in Fig. 1. We say that these lines belong to the same family. A family is in correspondence with an edge orientation. In a $D \to 2$ tiling, there are D edge orientations and therefore D families of de Bruijn lines.

The relevant object here is not the grid itself but the underlying intersection topology, which defines the tiling: a grid can be directly read on a tiling by joining together the middles of opposite edges, but it can

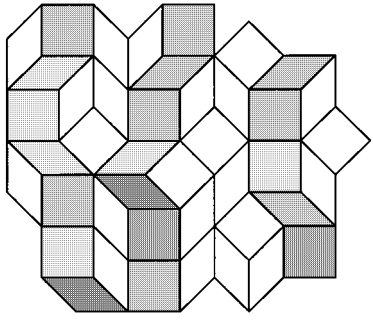

Fig. 1. A patch of octagonal $(4 \to 2)$ tiling. Some worms (de Bruijn lines) are represented. There are 4 families of worms. We have only drawn lines out of one of them (grayed).

afterwards be continuously deformed provided no triple point appears in the process. This grid and the tiling are said to be *dual*. In the following, we will sometimes distinguish between the terms "worms," which are sequences of rhombi of a tiling, and "de Bruijn lines," which are elements of a grid in an abstract grid space, with no underlying tiling any longer.

Conversely, it can be proven that, given such a grid, it is possible to build a unique tiling, the de Bruijn grid of which is identical to the grid under consideration.[15, 16, 18]

Two lines of two different families can but need not intersect. A grid where all lines of all families intersect is said to be *complete*. In this case, to insure the existence of all intersections, we impose that, "far" from the intersection region, the lines are perpendicular to vectors $\mathbf{u}_i$, one per family. The lines of a given family are therefore parallel at the infinity.

Directed faceted membranes are representations of tilings in hypercubic lattices of higher dimensions, which have been developed to study random tilings in parallel with the partition method (see below).[19, 11, 20, 3, 21, 22] They are the generalization of one-dimensional directed walks (or polymers) in hypercubic lattices. This point of view is closely related to the cut-and-project method. Therefore we shall only give a brief presentation of these membranes. The main idea is that a $D \to d$ random tiling can be lifted as a d-dimensional non-flat structure embedded in a D-dimensional space.

This structure is a *continuous membrane* made of d-dimensional facets of the $\mathbb{Z}^D$ hypercubic lattice. When this membrane is projected along the suitable direction, the projections of these facets are precisely the tiles the tilings are made of; its continuous character guarantees the absence of gaps in the so-obtained tiling. Such a membrane is said to be *directed* to emphasize the fact that its projection does not create any overlap. For example, Fig. 2 displays a $3 \to 2$ tiling, which can also be seen as a 2-dimensional non-flat directed membrane embedded in a cubic lattice. To get a tiling, this membrane must be projected along the (1, 1, 1) direction of the cubic lattice. This point of view can be generalized to arbitrary dimensions and codimensions. This correspondence is always one-to-one.

1.2. Partitions in Codimension One

It is possible to derive from this membrane representation a coding of random tilings by combinatorial objects called "partitions."[19, 20, 3, 21]

This point of view is easily understood when looking at Fig. 2: the membrane can be seen as a stacking of unit cubes in 3 dimensions and an integral height (the number of cubes) can be assigned to each of the kl columns of this stacking, resulting in a $k \times l$ array containing integers. Since the original membrane is directed, these numbers are decreasing in each

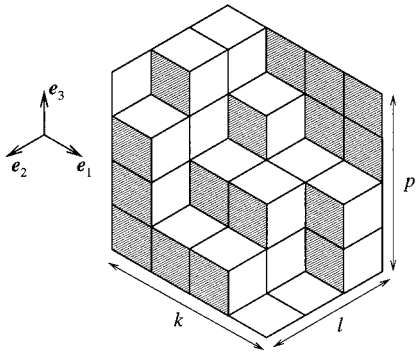

Fig. 2. 3-dimensional representation of a $3 \to 2$ tiling.

row and in each column of this two-dimensional array. This latter array is called a *plane partition* and each integer a *part*. In this representation, the integer p is called *the height* of the partition. It is the upper bound of each part. There is a one-to-one correspondence between such partitions and membranes embedded in a $k \times l \times p$ piece of cubic lattice. There is a straightforward generalization of this point of view to $D+1 \to D$ membranes and D-dimensional partitions (called *hypersolid partitions*), which are families of integers arranged in D-dimensional arrays, decreasing in each direction (for more complete details, see ref. 3, Sections 2.1 and 2.2).

In the following section, we generalize this partition point of view to any codimension tilings, which enables us to build their configuration space. This general point of view was only briefly tackled in previous refs. 11, 20, and 3. It was developed and formalized in ref. 21.

2. HIGHER CODIMENSIONS TILINGS

In this section, we show how it is possible to code octagonal tilings, or more generally $D \to d$ tilings, as *generalized partitions*, that is families of integral variables, but living on structures more complex than the previous rectangular arrays. These structures will turn out to be the dual graphs of relevant rhombus tilings.

2.1. Generalized Partitions

Our goal in this section is to prove that $D \to d$ tilings can also be coded by "generalized partitions on $(D-1) \to d$ tilings." Let us explain what this terminology means.

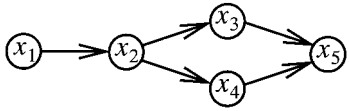

Fig. 3. A simple example of directed graph. It defines a partition problem. The associated partition problem has 5 variables, which are related by: $x_1 \geqslant x_2$; $x_2 \geqslant x_3$; $x_2 \geqslant x_4$; $x_3 \geqslant x_5$; $x_4 \geqslant x_5$.

Generally speaking, we define a *partition problem* as a family of K integral variables, denoted by $x_1, x_2, ..., x_K$, placed at the vertices of a directed graph, so that any two variables placed at two adjacent vertices satisfy an order relation in agreement with the orientation of the edge between those vertices.[4] The underlying directed graph is called the *base* of the partition problem. To simplify, we shall consider that all order relations are weak ($x_i \geqslant x_j$). The integral values are between 0 and an integer p, called the *height* of the partition problem. A solution of this problem is called a partition, of height p. The integral variables x_i are called the *parts*. Figure 3 displays an example. In ref. 3, we mainly studied hypersolid partitions, the graph of which is equivalent to a piece a hypercubic lattice, in the context of codimension-one partition problems (see above, Section 1.2).

To introduce the tiling coding by partitions, we shall work in the grid representation. We focus here on the $D \to 2$ case (the presentation of the general $D \to d$ case would require some more definitions and refinements. The interested reader will refer to refs. 21 and 23; see also Appendix D). Let us consider a $D \to 2$ grid. We single out a family of lines, which can be chosen as the Dth one without loss of generality. It contains k_D de Bruijn lines. The $D-1$ remaining families define a new grid. We call it a *subgrid* of the first one. Our goal is now to build a partition on this subgrid that codes the initial tiling: a part will be attached to each vertex of this subgrid.

Firstly, we need to introduce the so-called *interline indices*. Since they do not intersect, the k_D singled out lines divide the plane in k_D+1 domains. These domains are unambiguously labeled from 0 to k_D in the simplest way: two adjacent domains are labeled by two successive numbers which are increasing in the direction of $\mathbf{u}_D$ (as defined in Section 1.1). Now the value of the part attached to a subgrid vertex is simply equal to the interline index of the domain in which this subgrid vertex lies. The maximum height of these parts is k_D.

There is a more simple way of characterizing the order between these parts: since a de Bruijn line of the subgrid is transverse to all the lines of

[4] To begin with, we shall suppose this directed graph to be *acyclic*, that is to say there is no sequence of inequalities such as $x_{i_1} \geqslant x_{i_2} \geqslant \cdots \geqslant x_{i_q} \geqslant x_{i_1}$. The general case will be discussed in Appendix D.

the Dth family, the parts on this line are ordered in the same direction as the interline indices. Therefore we have defined a "canonical" order on every subgrid line. We say that we have ordered those de Bruijn lines. By convention, we chose those lines to be ordered in the direction of *decreasing parts* (we insist on this point because it is a source of confusion). Now, since any two adjacent vertices of the subgrid are joined by such a line, we have ordered any two parts. Therefore we have defined on this subgrid a partition problem of height k_D. To sum up, we have coded any $D \to 2$ grid as a pair: a $D-1 \to 2$ subgrid and a partition on it.

Conversely, given such a pair, the $D \to 2$ grid from which this pair comes can be easily re-constructed. One must add the Dth family of lines in such a way that all the vertices of the subgrid lie in the interline, the index of which is equal to the part attached to this vertex. The constraints on the parts insure that we actually obtain a $D \to 2$ de Bruijn grid.

In conclusion, we have derived a one-to-one mapping between $D \to 2$ grids and partitions on $D-1 \to 2$ subgrids, the parts being suitably ordered on oriented de Bruijn lines. A more mathematical formulation, related to this work, can be found in ref. 23.

This mapping can be translated in the tiling (or directed membrane) language: the generalized partitions can be defined on the suitably oriented dual graphs of the corresponding $D-1 \to 2$ tilings. For short, we call them "partitions on tilings."

Figure 4 provides an example of $4 \to 2$ tiling seen as a partition on a $3 \to 2$ tiling. The $3 \to 2$ tiling has been slightly deformed to anticipate the next step of the process. Note that parts are ordered on each de Bruijn line (or worm). Once the partition has been chosen, zones where parts are equal are separated by bold lines, which are "opened" to form worms (shaded) of width 1. This step is the manifestation in the tiling representation of the fourth de Bruijn family.

To conclude this paragraph, we shall say that a $D \to d$ tiling problem can be studied as a collection of partition problems on a set of (dual graphs

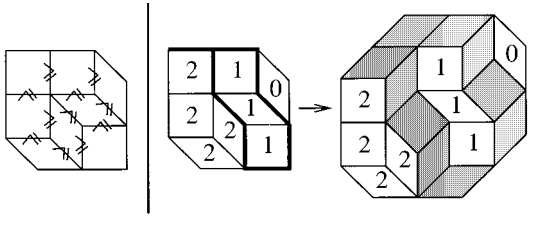

Fig. 4. A $4 \to 2$ tiling coded by a generalized partition on a $3 \to 2$ tiling. Left: the inequalities between the tiles. Right: a partition of height 2 and the corresponding $4 \to 2$ tiling. It fills an octagon of sides 2, 2, 2, 1.

of) $D-1 \to d$ tilings. Even though we have only proved this point in the $4 \to 2$ case, the demonstration can be generalized.[21] Practically, to build a $D \to d$ tiling, one can iterate a partition-on-tiling process. The first step is simply a codimension-one partition on a d-dimensional hypercubic array. It generates a $d+1 \to d$ tiling. The next steps increase D by one each. Therefore there are $D-d$ steps.

As compared to usual random tilings, partition-generated ones have specific polygonal boundary conditions. For example, the tiling in Fig. 2 have a hexagonal boundary. In the case of $4 \to 2$ tilings, the polygon is an octagon of sides k_1, k_2, k_3 and k_4 (see Fig. 4). More generally, such tilings have *zonotopal*[5] boundaries. Note that they are dual to complete de Bruijn grids. It should also be mentioned that such polygonal boundaries have a strong macroscopic influence on tilings, which results in a lower entropy than in free or periodic-boundary systems.[3, 22, 24, 25]

2.2. Configuration Space

In this section, we study the configuration space of partition-generated tilings that fill a given polygonal domain.

The codimension-one case has already been studied in detail:[3] the configuration space $\mathscr{C}$ consists of all the integral coordinate points (*integral points*) lying into the convex polytope defined by the system of inequalities related to the partition problem. This configuration space is embedded into an Euclidean space of dimension K, where K is the number of parts of the partition problem. Two points are neighbors in $\mathscr{C}$ (i.e., they are linked by an edge of the underlying hypercubic lattice) if they only differ by a local rearrangement of tiles which is usually called an (elementary) flip[3] (see Fig. 5).

In this section, all the latter properties are extended to generalized $4 \to 2$ problems, in particular to partitions-on-tiling problems. In ref. 21, the general $D \to d$ case is treated.

Let us consider $4 \to 2$ tilings which fill an octagonal region of sides k_1, k_2, k_3 and k_4. They are described by a class of partition problems on $3 \to 2$ tilings inscribed in hexagons of sides k_1, k_2 and k_3. These tilings will be indexed by an integer α. They have exactly $K = k_1k_2 + k_1k_3 + k_2k_3$ parts.

[5] The zonotope generated by the family of d-dimensional vectors $(\mathbf{v}_1, \mathbf{v}_2, ..., \mathbf{v}_D)$ is the set

$$Z = \left\{ \sum_{i=1}^{D} \alpha_i \mathbf{v}_i,\ 0 \leqslant \alpha_i \leqslant 1 \right\}$$

It is also called the *Minkowski sum* of vectors $\mathbf{v}_i$. In two dimensions, it is a $2D$-gon. The link between vectors $\mathbf{v}_i$ and the D-dimensional representation is specified in refs. 3 and 21.

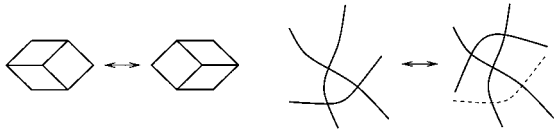

Fig. 5. An elementary flip (left) and its grid space counterpart (right).

Therefore each configuration space $\mathscr{C}_\alpha$ related to the partition problem on α is of dimension K. Now to describe the whole configuration space of the tiling problem, we need to make explicit how these different $\mathscr{C}_\alpha$ are connected to each other.

Firstly, we need to specify how a flip in the tiling representation is translated in the grid space. It is simply a 3-line flip, as illustrated in Fig. 5.

If the fourth family of lines has been singled out in the partitions-on-tiling process, two cases must be distinguished:

I: either the 3-line flip does not involve any line from the fourth family. It means that the 3 vertices involved in the flip have the same interline index and that this index does not evolve during the flip. These vertices are therefore coded by parts of same value. On the other hand, the base tiling (i.e., the tiling dual to the 3-family subgrid) on which the partitions are defined undergoes a flip;

II: or the flip involves a line l of the fourth family. In this case, the 3-family subgrid is not modified through the flip. The same holds for the base tiling on which the partitions are defined. On the other hand, let us consider the only vertex S involved in the flip but which does not belong to l. During the flip, its interline index is increased by ± 1. Therefore a part (and only one) of the partition problem varies (by ± 1).

To sum up, a flip is translated either in a base tiling flip, without any modification of the parts (type-I flip), or in a variation of one of the parts without any modification of the base (type-II flip).

Let us go back to the configuration space $\mathscr{C}$. Since $\mathscr{C}$ can be seen as a collection of spaces $\mathscr{C}_\alpha$ associated with tilings α, it can be given a "discrete fiber bundle"[6] structure, the base $\mathscr{B}$ of which is the configuration space of (base) tilings α. Its fibers are the spaces $\mathscr{C}_\alpha$.

Practically, suppose that $\mathscr{B}$ is embedded in an hypercubic array of dimension δ and that the dimension of each fiber is K. Then the whole space can be embedded in a lattice $\mathbb{Z}^\delta \times \mathbb{Z}^K$: the first δ coordinates code the base tilings α and the K last ones the parts on these tilings. We already know the structure of $\mathscr{C}$ inside a fiber: an edge between two vertices

[6] We employ improperly this term. In particular all the fibers are not necessarily identical.

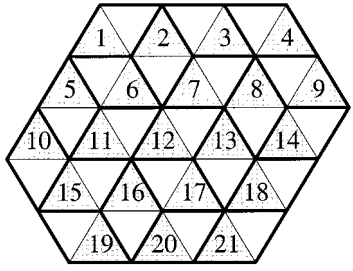

Fig. 6. A $3 \to 2$ tiling as a domino tiling on a triangular lattice. Each tile is labeled like its unique upward triangle.

corresponds to a type-II flip. Now, we must establish how a type-I flip connects two fibers.

A type-I flip consists of a flip in the base tiling, transforming the tiling α into α', but which does not alter the values of the parts. In the fiber, the K coordinates of the corresponding points are therefore unchanged. But in the base $\mathscr{B}$, α and α' are coded by two points which differ by only one of their δ coordinates. Thus, in $\mathscr{C}$, the two tilings differ by only one coordinate: they are neighbors in $\mathbb{Z}^\delta \times \mathbb{Z}^K$.

However, we have omitted to deal with a subtlety in the previous statement: so far, we have proven that two fibers are connected *via* a piece of hypercubic lattice. Thus we have only proven the *local* hypercubic structure of the configuration space. To provide a complete proof, we need to exhibit an extrinsic[7] set of hypercubic coordinates in which every configuration can be encoded and in which two neighbor tilings differ by a single flip. As a matter of fact, we only have to specify coordinates in fibers: the choice of coordinates in the base $\mathscr{B}$ is an irrelevant question. As it was stated above, a choice of coordinates is equivalent to the choice of a tile-labeling of a $3 \to 2$ base tiling. Now, as illustrated in Fig. 6, such a tiling can be seen as a domino tiling on a triangular lattice: every tile is the union of an upward and a downward triangle. Therefore any labeling of upward triangles will provide a tile-labeling and therefore a set of coordinates in each fiber. It is now clear that with such coordinates, a type-I flip corresponds to a bond of the hypercubic lattice.

Remark. We can now derive the dimension of the hypercubic lattice in which $\mathscr{C}$ is embedded:

$$d_{\mathscr{C}} = \delta + K = 2k_1k_2 + k_1k_3 + k_2k_3 \tag{1}$$

[7] That is independent of the fiber.

since the dimension of the base is k_1k_2 and the dimension of fibers is $k_1k_2+k_1k_3+k_2k_3$.

These arguments in the octagonal case can be extended by induction to the general $D \to d$ problem,[21] at least as far as the local hypercubic structure is concerned (see Appendix D).

Note also that, following this work, this configuration space has been recently investigated further by M. Latapy, who detailed the nature of its structure when it is seen as a partially ordered set,[26] in any $D \to 2$ case. Briefly speaking, the lattice structure in the fibers looks like that of a plane partition configuration space (it is a "distributive lattice"), whereas the structure of the whole set is a bit less rich (it is a lattice, but not a distributive one).

Another interesting question concerns the connectivity of this configuration space: for a given boundary, is it possible to obtain a random tiling from any other one *via* a sequence of elementary flips? In the $D \to 2$ case, the configuration space is connected for any D.[27, 28] The present analysis provides another straightforward proof of this result: every fiber is connected as the configuration space of a partition problem on an acyclic directed graph since it is the convex union of normal simplices. Moreover, the base is connected for the same reason (inductively), which completes the proof. The general case is discussed in Appendix D.

3. DECOMPOSITION OF THE CONFIGURATION SPACE INTO NORMAL SIMPLICES: GENERAL CASE

3.1. Simple Descent Theorem

We first recall the results of refs. 3 and 29 about generalized partitions. The configuration space of a generalized K-part partition problem of height p is embedded in a K-dimensional Euclidean space, the coordinates x_i of which are the parts of the problem. The configurations are coded by integral-coordinate points (called integral points), which belong to the convex polytope $\mathscr{F}^{[K]}$ defined by the intersection of the hypercube $(0 \leqslant x_i \leqslant p)$ and of the cone $(x_i \leqslant x_j)$ defined by all the suitable relations between the parts.

The key point is that this configuration space can be decomposed into elementary volumes, the so-called *normal simplices*. Let $(\mathbf{e}_1, \mathbf{e}_2, ..., \mathbf{e}_K)$ be the orthonormal basis of the Euclidean space which generates the $\mathbb{Z}^K$ lattice. A K-dimensional simplex of vertices $A_0, A_1, ..., A_K$ is said to be *normal* if there exists an integer s such that:

- each A_i is an integral point,

- A_iA_{i+1} is parallel to a vector $\mathbf{e}_{k_i}$ for any i,
- if $i \neq j$ then $k_i \neq k_j$,
- $\|A_iA_{i+1}\| = s$ for any i.

For short, we shall call such a simplex a *normal simplex of side s*. Its integral volume (i.e., the number of integral points it contains) can easily be derived: it is the binomial coefficient $\binom{s+K}{K}$. But such simplices have lower-dimensional faces in common that contain integral points, which must not be double-counted. Therefore we must take into account a subtle inclusion-exclusion scheme in order to count correctly the number of configurations. To sum up, one must suppress j faces ($j = 0,..., j_{\max}$) to some simplices in order to avoid double-counting. If a_j is the number of simplices that lose j faces, then the number of configurations is

$$W(p) = \sum_{j=0}^{j_{\max}} a_j \binom{p+K-j}{K} \tag{2}$$

where the maximum number of suppressed faces, $j_{\max}$, depends on the partition problem under study.

The so-called *descent theorem*[3] provides a prescription to characterize the coefficients a_j. To state this theorem, we need the following definition: with each simplex of the decomposition, we can associate the sequence $(k_1,..., k_K)$ of indices appearing in the definition of the normal simplex. Then *the number of descents* in this sequence is the number of indices such that $k_i > k_{i+1}$.

The descent theorem states that, if there exists a zero-descent simplex, which is always true up to a re-indexing of the basis vectors,[8] then a simplex with j descents loses j faces. Therefore the coefficient a_j in Eq. (2) is equal to the number of simplices with j descents.

As a corollary, the number of normal simplices in the decomposition is equal to the sum of the coefficients a_j of Eq. (2).

These coefficients a_j can be given a different equivalent interpretation:[3, 29] one builds a directed graph, denoted by T, with two extremal vertices, O and S_0. A simplex of the decomposition is put in one-to-one correspondence with *maximal* walks in T (i.e., going from O to S_0). More precisely, to each vertex of the graph, it corresponds a configuration of height $p = 1$ of the partition problem. Two configurations are neighbors if they differ by only one part x_i, which is 0 in the "lower" configuration and 1 in the "higher." Therefore the link between the two configurations can be

[8] At least in the case of an acyclic base graph (see Appendix D).

indexed by i and the descent theorem can be translated in terms of these indices: the number of descents of a walk in the graph is defined as the number of descents of the sequence of indices of the bonds it follows.

To sum up, in the graph T of any generalized partition problem, a step between a vertex and one of its neighbors in a maximal walk amounts to increasing one of the parts from 0 to 1. Therefore a maximal walk from O to S_0 amounts to a labeling of the parts, from 1 to K, which specifies in which order they are increased from 0 to 1. O (resp. S_0) is the configuration where all the parts are equal to 0 (resp. 1).

In codimension-one $D+1 \to D$ partition problems, we have proved that the graph T is the configuration space of the $D \to D-1$ partition problem on a hypercubic array of sides $k_1, k_2, ..., k_{D-1}$.[3]

In codimension larger than one, that is in the case of partition-on-tiling problems, the parts are attached to the tiles of the $D-1 \to d$ problem, as in Fig. 4. Therefore, to each maximal walk in the graph T, it corresponds a labelling of the tiles, which characterizes in which order the parts are increased by one in the walk.

For example, Fig. 8 (left) shows a tile labeling (among many others) in the partition problem of Fig. 7 (left). In fact, the only condition on those labelings is that when two tiles x_i and x_j are adjacent, if the order relation is $x_i \geqslant x_j$, the label associated with x_i is *smaller* that the label associated with x_j (x_i is increased *before* x_j). In other words, these labels are ordered on de Bruijn lines.

3.2. Decomposition in Simplices

A $4 \to 2$ tiling problem is a collection of generalized partition problems on $3 \to 2$ tilings. On each such tiling, the descent theorem can be applied. Therefore, the counting polynomial of the $4 \to 2$ problem, which is the sum of all the individual polynomials on each $3 \to 2$ tiling, can also be written

$$W = \sum_{j=1}^{M} a_j \binom{p+K-j}{K} \tag{3}$$

where K is the number of tiles, independent of the $3 \to 2$ tiling, and M is the greater of the integers $j_{\max}$ involved in the collection of partition-on-tiling problems.

In this section, we shall prove that the above result for codimension-one problems[3] can be generalized: the sum of the coefficients a_j of the counting polynomial W is equal to the number of maximal walks of a given

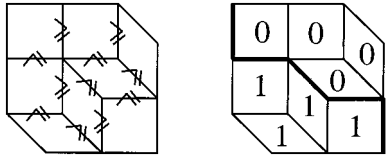

Fig. 7. A partition problem on a $3 \to 2$ tiling. Left: $\geqslant$ symbols show the order relations between tiles. We recall that parts are canonically ordered on each worm. Right: a solution of height $p = 1$ and the line separating 0's and 1's. Note that this line has been extended up to the top-left and bottom-right corners of the hexagon. As a matter of fact, this line is the projection of a $3 \to 1$ tiling.

class in the related configuration space of a given $3 \to 1$ tiling problem. At the end of this section, we shall give an explicit analytic expression of this number of walks.[21] A general result concerning walks in the configuration space can be derived in the general $D \to d$ case. However, to avoid inessential complication, we shall present it in the restricted $4 \to 2$ case, and in an informal manner. A rigorous proof in the $D \to 2$ case is given in Appendix A and the general case is discussed in Appendix D.

Let us consider a partition problem on a $3 \to 2$ membrane, or, equivalently, on a $3 \to 2$ tiling. Figure 7 (left) provides an example.

As we have seen it at the beginning of this section, the sum of the coefficients a_j of this (generalized) partition problem is equal to the number of labelings of the tiles, with integers running from 1 to K, which respect the following condition: these labels must be increasing on each oriented de Bruijn line. Figure 8 (left) displays such a labeling in the case of the $3 \to 2$ tiling of Fig. 7.

On the other hand, a configuration of this partition problem of height $p = 1$ is characterized by the line which separates 0's and 1's on the tiling. Figure 7 (right) shows a partition of height 1 and the corresponding line. In Fig. 8 (right), some other such line configurations, associated with partitions of height 1, are displayed. These lines are directed walks using three kinds of elementary steps: north, west and north-west ones. The number of steps in each direction is determined by the side lengths of the hexagonal boundary.

Now, a walk in the space of partitions of height 1 is also a walk in the space of these directed lines. For example, the walk of Fig. 8 (left) is encoded into the sequence of lines of Fig. 8 (right). On the other hand, we notice that these latter lines can be seen as projections in two dimensions of $3 \to 1$ directed membranes (i.e., one-dimensional walks embedded in a cubic lattice). These membranes lie on the same rectangular parallelepiped as the initial $3 \to 2$ membrane. A walk counted by the sum of the coefficients

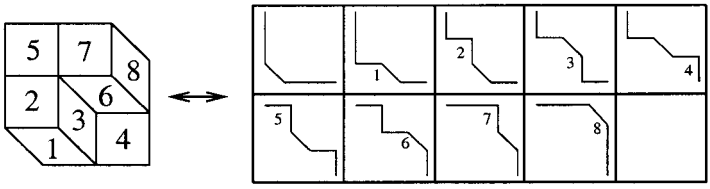

Fig. 8. Left: a walk in the configuration space of the partition problem on the $3 \to 2$ membrane encoded by a labeling of the 8 tiles of this membrane. This labeling respects the order on the de Bruijn lines. Right: the walk in the $3 \to 1$ problem configuration space associated with the left-hand-side labeling. One goes from a broken directed line to the next *via* a single flip. The extremal tilings are the first and the last ones.

a_j of the partition problem on this membrane is therefore also a walk in the configuration space of a given class of $3 \to 1$ membranes.

To sum up, the sum of the coefficients a_j of this partition problem is equal to the number of ways of labeling the partition parts with some rules. Such a labeling can be put in correspondence with walks in a suitable configuration space of $3 \to 1$ tilings. And the same holds for each individual partition problem on a $3 \to 2$ tiling.

Conversely, given such a walk it is always possible to reconstruct the $3 \to 2$ tiling it comes from, as well as the labeling on this tiling. Therefore this walk is counted by the sum of the coefficients a_j of a partition problem on a $3 \to 2$ tiling, hence by the sum of the coefficients a_j of the initial $4 \to 2$ tiling problem.

In conclusion—and we rigorously prove this result in Appendix A—the sum of the coefficients a_j of a $4 \to 2$ tiling problem is equal to the number of maximal walks in the configuration space of a suitably related $3 \to 1$ tiling problem.

Theorem. For any problem of enumeration of fixed boundary $4 \to 2$ tilings, the sum of the coefficients a_j of the additive counting polynomial

$$W^{4\to 2}(p) = \sum_{j=0}^{M} a_j \binom{p+K-j}{K} \tag{4}$$

is equal to the number of maximal walks in the configuration space of the associated $3 \to 1$ tiling problem (as defined in Appendix A).

Generalizing codimension-one notions, by "maximal walk," we mean a walk between two tilings which play a singular role in the configuration space, the so-called "extremal" tilings (Fig. 8). One of the properties of

these extremal tilings is that they go in pairs and that the (Manhattan) distance between two such configurations is a local maximum in the configuration space, even in the general $D \to d$ case.[21] These tilings are described in Appendix A and Appendix D (see Figs. 12 and 24).

In Appendix B, we explicitly calculate this number of walks in the $D \to 1$ configuration spaces. In particular, if $A_3(k, l, m)$ denotes the sum of the coefficients a_j of the polynomial counting the number of $4 \to 2$ tilings inscribed in an octagon of sides (k, l, m, p),

$$A_3(k, l, m) = (kl + km + lm)! \frac{[(l-1)!^{[2]}]^2}{(2l+k+m-1)!^{[2]}} \times \frac{(k-1)!^{[2]}\,(m-1)!^{[2]}\,(2l+k-1)!^{[2]}\,(2l+m-1)!^{[2]}}{(2l-1)!^{[2]}\,(l+k-1)!^{[2]}\,(l+m-1)!^{[2]}} \tag{5}$$

where we have used the *generalized factorial functions* of order 2, as defined in ref. 20: $k!^{[2]} = \prod_{j=1}^{k} j!$. Some properties of these functions are given in ref. 3.

3.3. Generalized Descent Theorem

As it was done in ref. 3 in the codimension-one case, we shall now refine the previous theorem in order to characterize among the maximal walks those which are counted by a given coefficient a_j.

In other words, we are looking for a descent theorem in any codimension. As in codimension one, we need an edge labeling in the associated $3 \to 1$ configuration space such that a_j is the number of maximal walks which have exactly j descents with respect to this labeling.

Now, we know that such an edge in the configuration space is in one-to-one correspondence with a facet of a $3 \to 2$ tiling (the value of which changes from 0 to 1). This two-dimensional facet also belongs to a membrane attached to the rectangular parallelepiped P. Therefore it belongs to the piece of cubic lattice bounded by P.

If we choose a labeling of all these two-dimensional facets bounded by P, it will induce a labeling of the facets of any $3 \to 2$ membrane attached to P. Such a labeling will be used to index the variables of the partition problem on this membrane. For example, Fig. 9 displays a labeling of the facets bounded by P, and Fig. 10 shows the induced labeling on a membrane attached to P. Then, according to the descent theorem, if there exists a zero-descent walk for this labeling, then a coefficient a_{j_0} of this individual

partition problem counts the number of j_0-descent walks on this membrane, and thanks to the correspondence between facets and edges, a j_0-descent in the whole $3 \to 1$ configuration space.

Conversely, let us consider any j_0-descent maximal walk in this configuration space. This walk is counted by the sum of the coefficients a_j of the partition problem on an individual $3 \to 2$ membrane. If there exists a zero-descent walk on this membrane, this walk is more precisely counted by the coefficient a_{j_0}.

In conclusion, we are looking for a labeling of the facets which induces, on any $3 \to 2$ membranes, a labeling with a zero-descent walk. Then the number of j_0-descent walks in the $3 \to 1$ configuration space will be equal to the coefficient a_j of the polynomial $W(p)$. We propose such a labeling in the following paragraph.

Let P be a rectangular parallelotope of sides $k_1 \times k_2 \times k_3$ embedded in a 3-dimensional lattice, the orthogonal basis of which is $(\mathbf{e}_1, \mathbf{e}_2, \mathbf{e}_3)$ (see Fig. 9; among all the possible choices, the hexagonal non-flat frame of the membranes is chosen as follows: it contains the vertices $(0, 0, k_3)$ and $(k_1, k_2, 0)$ of P). Each facet is coded by the coordinates of its center. We define on these coordinates an order relation $\prec$ close to the lexicographic

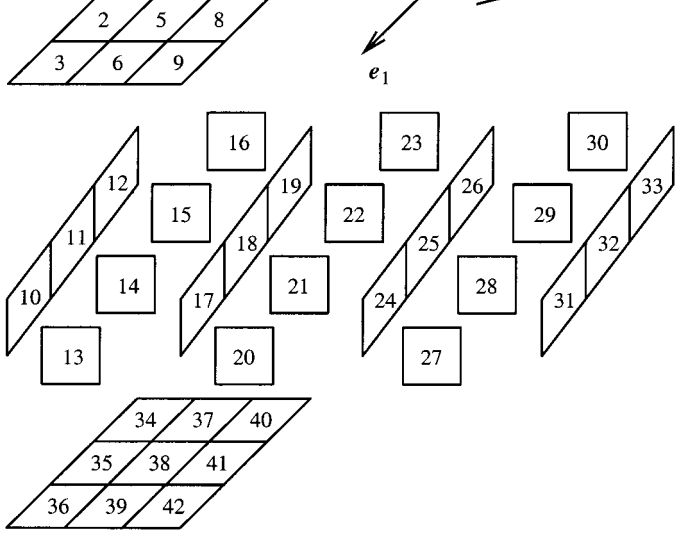

Fig. 9. Labeling of the two-dimensional facets of a parallelepiped P of sides $3 \times 3 \times 1$. For any k_3 larger that 1, the same labeling could be handled in the same way.

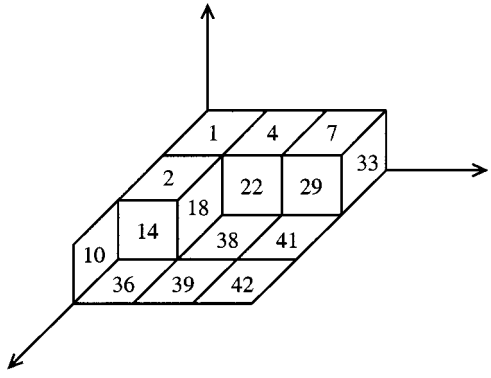

Fig. 10. Example of labeling induced on a $3 \to 2$ membrane.

order, apart from a slight difference: let f_1 and f_2 be two facets, the center coordinates of which are respectively (x_1^1, x_2^1, x_3^1) and (x_1^2, x_2^2, x_3^2). Then

- if $x_3^1 > x_3^2$ then $f^1 \prec f^2$.
- if $x_3^1 = x_3^2$ and this value is an integer, i.e., these facets are horizontal,[9] then
  - — if $x_2^1 < x_2^2$ then $f^1 \prec f^2$.
  - — if $x_2^1 = x_2^2$ and if $x_1^1 < x_1^2$ then $f^1 \prec f^2$.
- if $x_3^1 = x_3^2$ and this value is a half-integer, i.e., these facets are vertical, then
  - — if $x_2^1 < x_2^2$ then $f^1 \prec f^2$.
  - — if $x_2^1 = x_2^2$ and if $x_1^1 > x_1^2$ then $f^1 \prec f^2$ (only this point differs from the lexicographic order definition).

Figure 9 illustrates this point. It displays a facet labeling compatible with the previous order relation. P has been "exploded" to enable a better reading. Let us emphasize the difference between horizontal and vertical layers.

In Fig. 10, we have represented a $3 \to 2$ membrane attached to P and its facet labeling induced by the previous one. We check that this labeling is compatible with the order on the de Bruijn lines (which are oriented from top to bottom here). This result does not depend on the chosen $3 \to 2$ membrane.

[9] Normal to $\mathbf{e}_3$.

Note that the so-obtained labelings differ from those previously defined in order to prove the hypercubic character of the configuration space (Section 2.2).

This establishes the existence of a descent theorem in the octagonal case of interest. It will be used in the following section to get finite tiling enumerations.

Remark. It is natural to wonder if there exists such a result in the general $D \to d$ case. Except the facet labeling, the same arguments hold in this general context: if such a labeling existed, it would provide a descent theorem. However, we have good reasons to believe that such a labeling does not exist. Indeed its existence would mean that in the general case, the counting polynomial can still be written $W(p) = \sum a_j \binom{p+K-j}{K}$. But we know examples (in the $7 \to 3$ case) where such an expression is false (see Appendix D). Therefore if there exists a general descent theorem, it will have a more complex statement than the previous one.

4. ENUMERATION RESULTS

4.1. Two Exact Formulas

In ref. 28, Elnitsky provides two exact formulas for $4 \to 2$ tiling enumeration, in the case where two sides of the octagon are equal to 1.

As displayed in Fig. 11, two cases must be considered, according to whether the two sides of length 1 are adjacent or not:

$$W^{4\to 2}_{r,1,s,1} = \sum_{a+b=r} \sum_{c+d=s} \binom{a+c}{a}\binom{b+c}{b}\binom{a+d}{a}\binom{b+d}{b} \tag{6}$$

$$W^{4\to 2}_{r,s,1,1} = \frac{2(r+s+1)!\,(r+s+2)!}{r!\,s!(r+2)!\,(s+2)!} \tag{7}$$

The sketches of the proofs of these formulas are recalled in Appendix C.1.

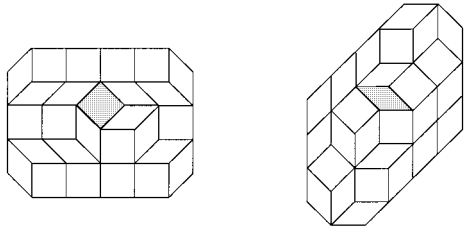

Fig. 11. Two tilings of octagons of sides r, 1, s, 1 (left) and r, s, 1, 1 (right).

In his paper, Elnitsky also says that no closed formula is known for the first double sum. We have somewhat simplified the first formula:

$$W^{4\to 2}_{r,1,s,1} = \frac{(r+s+1)!}{r!\,s!(2r+1)(2s+1)}\left[\frac{2(r+s+1)!}{r!\,s!} + \sum_{k=0}^{r}\frac{1}{2k-1}\binom{r}{k}\binom{s}{k}\right] \tag{8}$$

Since the last sum can be written in terms of a hypergeometric function

$$\sum_{k=0}^{r}\frac{1}{2k-1}\binom{r}{k}\binom{s}{k} = {}_3F_2[-1/2,\ -r,\ -s;\ 1/2,\ 1;\ 1] \tag{9}$$

this result is a "closed" form for the enumerating function, even though it is not written in terms of products or ratios of simple functions.

In order to prove Eq. (8), we need the following recursion relation, due to Brock:[30]

$$W^{4\to 2}_{r,1,s,1} - W^{4\to 2}_{r-1,1,s,1} - W^{4\to 2}_{r,1,s-1,1} = \binom{r+s}{r}^2 \tag{10}$$

The sketch of the proof of this recursion relation is also given in Appendix C.2.

If the right-side member of Eq. (8) is written as the sum of two terms, we denote the first one by $A_{r,s}$ and the second one by $B_{r,s}$. Then

$$A_{r,s} - A_{r-1,s} - A_{r,s-1} = \binom{r+s}{r}^2\left[1 + \frac{1-4rs}{(4r^2-1)(4s^2-1)}\right] \tag{11}$$

by simple algebraic manipulations, and

$$\begin{aligned} B_{r,s} - B_{r-1,s} - B_{r,s-1} &= \binom{r+s}{r}\frac{1}{(4r^2-1)(4s^2-1)}\sum_{k=0}^{r}\frac{1}{2k-1}\binom{r}{k}\binom{s}{k} \\ &\quad\times\left[(2r-1)(2s-1)(r+s+1) - r(2r+1)(2s-1)\frac{r-k}{r}\right. \\ &\quad\left. - s(2s+1)(2r-1)\frac{s-k}{s}\right] \\ &= \binom{r+s}{r}\frac{4rs-1}{(4r^2-1)(4s^2-1)}\sum_{k=0}^{r}\binom{r}{k}\binom{s}{k} \\ &= \binom{r+s}{r}^2\frac{4rs-1}{(4r^2-1)(4s^2-1)} \end{aligned} \tag{12}$$

since the last sum is equal to $\binom{r+s}{r}$, which proves that our expression satisfies relation 10. Since it also gives the expected values for $r=0$ or $s=0$, this achieves the proof.

Note however that those two formulas do not give any relevant information on the entropy since r and s the bigger, the most the tiling looks like a square lattice, with two defect lines (the two worms of the two other families) that only have a linear contribution to the entropy. Therefore the entropy per tile vanishes when r and s tend to infinity.

4.2. Numerical Results

In Table I, we list some coefficients a_j obtained *via* the method exposed above: we construct the oriented graph of the configuration space of the corresponding $3 \to 1$ problem and apply the generalized descent theorem, as described in the codimension-one case in ref. 3. Its label is attached to each (oriented) edge of the graph of this configuration space,

Table I. Coefficients a_j Associated with Some Octagonal Tiling Problems

k_1, k_2, k_3	$a_0; a_1;...$
2, 2, 2	20; 220; 703; 943; 566; 166; 21; 1
3, 2, 2	50; 1281; 9775; 32304; 53175; 46343; 22095; 5755; 774; 47; 1
2, 3, 2	50; 1240; 10472; 40378; 77328; 75652; 36506; 7958; 648; 18
2, 3, 3	175; 9792; 183223; 1611390; 7581596; 20313994; 31942744; 29678550; 16076840; 4906164; 794328; 62142; 2088; 24
3, 2, 3	175; 10372; 184113; 1445070; 5924665; 13826440; 19251677; 16431348; 8710059; 2861124; 569191; 65214; 3943; 108; 1
3, 3, 3	980; 119284; 4736040; 88959048; 922861456; 5735679224; 22400451966; 56586512056; 93968296600; 103217016568; 74801020694; 35369632364; 10693166706; 2003702920; 222619576; 13801976; 439638; 6272; 32
3, 3, 4	4116; 990574; 75291817; 2672974232; 52557540678; 628628119744; 4845859698991; 25007135636872; 88641414434386; 219565301033744; 384158453148998; 477331133707230; 421472964232612; 263431654905354; 115559997005453; 35098071282418; 7238626577471; 987285691504; 85977846450; 4564265102; 138792310; 2208928; 15936; 40
3, 4, 4	24696; 11185183; 1658701257; 117639867825; 4696728888239; 115554431503049; 1855639954964533; 20237165017326054; 154261056214441072;...
4, 4, 4	232848; 211868010; 59911555328; 7889440518518; 578616346951691; 26140019431942187; 775751817756005455; 15811577667366075305;...
4, 5, 5	16818516; 52683466776; 49453853710872; 21112489152560570; 4940628646460445115; 704860523557345706986; 6567632267357910687 2954;...
5, 5, 5	267227532; 1658888888852; 2898208633474138; 2212967878070760376; 903353585201401013350; 221402610595368245987868;...

Table II. Some Tiling Enumerations Computed with the Previous Coefficients and the Corresponding Entropies per Tile. We Have Only Listed Diagonal Entropies. The Number of Rhombi Is Given in Column 3

k_1, k_2, k_3, k_4	Number of tilings	# tiles	Entropy
1, 1, 1, 1	8	6	0.34657
2, 2, 2, 2	5383	24	0.35796
3, 3, 3, 3	273976272	54	0.35979
4, 4, 4, 4	1043065776718923	96	0.36022
5, 5, 5, 5	296755610108278480324496	150	0.36031

as prescribed in the generalized descent theorem scheme, and the coefficients a_j are computed recursively: if $a_j(v)$ is the number of walks in the configuration space from the extremal vertex O to the vertex v, with j descents, then the sequence $(a_j(v))_{j=0,\ldots,j_{\max}}$ only depends on the vertices under v in the graph. Then the coefficients we are interested in are equal to $a_j(S_0)$, where S_0 still denotes the extremal vertex associated with O.

One checks that the corresponding sums $\sum a_j$ are in agreement with those computed in Section 3.2 (Eq. (5)). Note that in Table I, the symmetry $a_j = a_{M-j}$ observed in codimension one is lost (M is the maximum number of descents). Indeed, this symmetry remains valid for each partition on tiling problem, but the maximum number of descents depends on the base tiling.

The derived counting polynomials provide enumerations of tilings, as well as entropies per tile[10] of finite-size systems. Some examples are listed in Table II. The interest of the method is that it gives access to enumeration of tilings for arbitrarily large k_4, if k_1, k_2 and k_3 are fixed. Moreover it is technically much easier to implement than a brute force enumeration method, and very much faster as well, in terms of computational time.

Even though it is not possible to make any reliable fit with few finite-size values, it is rather clear from the available data that the diagonal[11] entropy converges rapidly to its limiting value. Note that in the $2 \to 1$ case as well as in the $3 \to 2$ one, where exact enumeration formulas are known (see ref. 3 for a review, for instance), the asymptotic behavior of the finite-size corrections to the entropy can be derived: they decrease like $\log(k)/k$. Fitting such a behavior with the numerical values, we get a limiting diagonal entropy close to $S = 0.36(1)$. The precision of this entropy cannot

[10] We recall that the entropy per tile is $S = \ln W/N$ where W is the number of configuration (tilings) and N the number of tiles.

[11] The entropy is said to be diagonal when all the boundary side lengths k_i are equal.

be refined beyond the second digit with the small amount of values we have got.

Previous entropy calculations *via* transfer-matrix methods where derived concerning octagonal tilings, but in the case of periodic or free boundary conditions,[5] leading to a limiting value $S = 0.434$. The difference between both results is due to the strong macroscopic effects of boundary conditions in those random tiling systems.[19, 22]

CONCLUSION

Among the large class of random tilings, this paper is devoted to fixed boundary codimension-two tilings of rhombi ("octagonal tilings"). We have established combinatorial properties of the configurational spaces of such tilings, extending results previously derived in the more restricted case of codimension-one tilings. Octagonal tilings are more closely related to real quasicrystals than are codimension-one tilings. Moreover, many of the results presented here can (at least partially) be extended to two-dimensional tilings of rhombi of any codimension, and even to any-dimensional tilings.

The present analysis provides additive formulas which simplify significantly the enumeration of finite-size tilings. In a geometrical viewpoint, these formulas come from a decomposition of the configuration space into elementary volumes, called normal simplices. The number of configurations in each of these simplices is known. But it is necessary to take into account interfaces between those volumes to avoid multiple counting, which is achieved by the generalized descent theorem. The number of simplices in this decomposition is also derived in the general two-dimensional case: these simplices are put in one-to-one correspondence with a class of paths in a configuration space of tilings of same codimension, but smaller dimension, which can be counted.

The new insight on the sets of octagonal tilings provided by this analysis will be useful to study topics such as diffusion in these configuration spaces, which is directly related to the rate of convergence of flip dynamics towards the equilibrium distribution. This problem has already been treated in the case of hexagonal tilings,[31–34] but is still an open question in higher codimension plane tilings. Significant progress will be published separately. It would also be of high interest to understand how the introduction of energetic interactions between tiles is translated in the configuration space and how it modifies the dynamics. Indeed, a realistic model of quasicrystals requires one takes into account energy, which can be in first approximation modeled by tile interactions; glass-like slow

dynamics are likely to appear in this case,[35, 36] even though no glassy behavior has been explicitely exhibited in rhombus tilings yet.[37, 38]

APPENDIX A. COEFFICIENTS a_j AND MAXIMAL WALKS IN CONFIGURATION SPACES

We consider $D \to 2$ fixed boundary tilings, described as generalized partitions of height k_D on $D-1 \to 2$ membranes or tilings. To each such membrane is attached a partition problem, and therefore a set of coefficients a_j. The sum of the coefficients a_j of the counting polynomial of all these $D \to 2$ tilings is equal to the sum, running over all the relevant $D-1 \to 2$ membranes, of the sums of the coefficients a_j on each such membrane.

Consider first a $D-1 \to 2$ membrane, denoted by $\mathscr{M}$, and a partition problem on $\mathscr{M}$. According to results of Section 3.1, the sum of the coefficients a_j of this partition problem is equal to the number of walks, in the configuration space of the partition problem of height 1, between two *extremal* $D-1 \to d$ configurations, O and S_0. All the parts are of O and S_0 are respectively equal to 0 and 1. Such a walk is denoted by a sequence $O = P_0, P_1, ..., P_{K-1}, P_K = S_0$.

We use again the grid representation of tilings and the formalism introduced in Section 2.1: the partition problem on $\mathscr{M}$ is seen as a partition problem on the vertices of the corresponding grid (which has $D-1$ families), $\mathscr{G}$, called the subgrid of the problem. The vertices of $\mathscr{G}$ are ordered on each de Bruijn family. A partition P_i of height $p=1$ consists of marking each vertex of $\mathscr{G}$ by a 0 or a 1. The vertices marked with a 0 and those marked with a 1 are separated by the only de Bruijn line of the Dth family of the original grid. This latter line is denoted by $\mathscr{S}_D$. Our goal is now to encode $\mathscr{S}_D$ by a $D-1 \to 1$ grid, or in other words by a $D-1 \to 1$ tiling.

Now the section of the subgrid $\mathscr{G}$ by $\mathscr{S}_D$ is precisely of this type. Indeed, if we identify the intersection of a de Bruijn line of the k_ith family and $\mathscr{S}_D$ with a i-tile, this latter section is a sequence of tiles, k_i of each family i, that is to say a $D-1 \to 1$ tiling.

Therefore the sequence (P_i) is coded by a sequence (C_i) of such tilings, as illustrated in Fig. 12. Since the same argument can be applied to any subgrid $\mathscr{G}$ of this $D \to d$ problem, all the walks counted by the sum of the coefficients a_j of the counting polynomial can be seen as such sequences (C_i).

It is now rather clear that all the configurations $C_0 = O$ and $C_K = S_0$ are the same for the partition problems on all subgrids $\mathscr{G}$: they are the two configurations where all the tiles of a same family are adjacent and where the families are ordered according to the grid configuration at infinity,

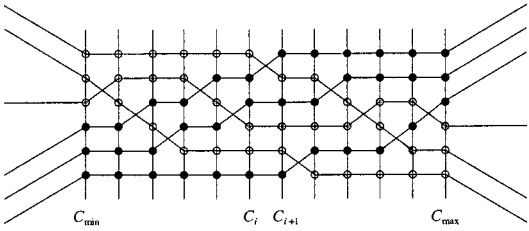

Fig. 12. Left: A $D-1 \to 2$ grid and the successive sections C_i by a line of the Dth family. Each section can be seen as a $D-1 \to 1$ tiling where the different species of tiles are represented by dots of different colors. Two successive sections differ by a single flip, that is the exchange of two tiles. In this example, $D=4$, $k_1=3$, $k_2=1$ and $k_3=2$. Right: The corresponding labeled dual tiling.

which does not depend on $\mathscr{G}$, but only on the vectors $\mathbf{u}_i$. These two configurations will be denoted by $C_{\min}$ and $C_{\max}$, as in Fig. 12. Likewise, two successive tilings of a sequence, C_i and C_{i+1}, only differ by a tile flip, that is the exchange of two adjacent tiles, since the two successive sections "surround" a single vertex of $\mathscr{G}$. And there is a natural order between two successive such tilings: considering how tiles are ordered on $C_{\min}$ and $C_{\max}$, it is clear which tiling should come first in the sequence.

Conversely, let us establish that such a sequence (C_i) of $D-1 \to 1$ tilings, going from $C_{\min}$ to $C_{\max}$, and where two successive tilings only differ by a single flip and respect the above order, contributes towards the sum of the coefficients a_j of a unique partition problem on a $D-1 \to 2$ membrane—and therefore towards the sum of the coefficients a_j of the global $D \to 2$ problem. The proof is rather straightforward and is also illustrated in Fig. 12: considering two successive tilings, C_i and C_{i+1}, the two dots that represent the two flipping tiles of different families are joined by two crossing segments; the so-obtained vertex is labelled by $i+1$; all the other tiles are joined by horizontal segments. Then one reconstructs a complete $D-1 \to 2$ grid, the vertices of which are labeled by numbers increasing on each de Bruijn line. This is precisely the kind of object counted by coefficients a_j.

Note that all the walks counted by $\sum a_j$ have the same length, since all the subgrids $\mathscr{G}$ have the same number of intersections.

APPENDIX B. NUMBER OF MAXIMAL WALKS IN A $n \to 1$ CONFIGURATION SPACE

In this section, we derive the number $A_n(k_1,\ldots,k_n)$ of walks $(P_i)_{i=0,\ldots,K}$ in the $n \to 1$ configuration space. Note that for sake of simplicity, we note n instead of $D-1$. We shall prove that:

$$A_n(k_1,\ldots,k_n)=\left(\sum_{1\leqslant i<j\leqslant n} k_ik_j\right)!$$
$$\times\prod_{1\leqslant i<j\leqslant n}\frac{(K_{ij}+k_i-1)!^{[2]}\,(K_{ij}+k_j-1)!^{[2]}}{(K_{ij}+k_i+k_j-1)!^{[2]}\,(K_{ij}-1)!^{[2]}} \qquad \text{(B.1)}$$

where $K_{ij}=2(k_{i+1}+\cdots+k_{j-1})$ when $i<j$.

We give two proofs: a purely algebraic one in the general case, using results by Stanley,[39] and a combinatorial one.[21] Note that the case where all the parameters k_i are equal to 1 was already treated by Stanley,[39] and that Edelman and Greene derived a nice combinatorial proof in this case.[40] We suppose that the notions of Young tableaux and standard Young tableaux are known.[12]

But before all, we need to introduce the relation between the tilings considered in this paper and a class of computer science objects, the so-called *sorting algorithms*. This analogy will help the presentation of the algebraic proof and will be useful in the combinatorial proof.

Appendix B.1. Tilings and Primitive Sorting Algorithms

In the sorting language, a *comparator* $[i;\,j]$ acts on a list $(x_1, x_2,\ldots, x_n)$ of numbers as follows: x_i and x_j are respectively replaced by $\min(x_i, x_j)$ and $\max(x_i, x_j)$. Following Knuth,[42] we call a *complete* sorting algorithm a sequence of such comparators which sorts in the increasing order any list of real numbers $(x_1, x_2,\ldots, x_n)$. This sorting algorithm will be called *primitive* if each comparator can be written $[i, i+1]$. We also suppose that this algorithm is not redundant, that is to say it does not contain any comparator $[i, j]$ that could be suppressed because previous comparators already insure that $x_i\leqslant x_j$. Knuth shows that a sequence of comparators is a sorting algorithm if it correctly sorts the completely reversed list $(n, n-1,\ldots, 1)$. This means that a complete primitive sorting algorithm is a sequence of comparators $[i, i+1]$ that transforms the list $(n, n-1,\ldots, 1)$ into the list $(1, 2,\ldots, n)$.

Such an algorithm can have a diagrammatical representation as follows: the n variables x_i are represented by n horizontal lines. Each comparator $[i, i+1]$ is represented by a crossing $\times$ between lines i and $i+1$.

[12] A Young tableau is a stacking of square boxes on a line, as displayed in Fig. 16 (left), with the only constraint that the number of boxes in columns decreases from left to right. The shape of the tableau is the decreasing sequence of the column heights. A standard Young tableau of a given shape is simply a numbering of the cells of the tableau by integral numbers, running from 1 to the number of cells and increasing in rows and columns. Figure 16 provides examples. For a presentation in relation with the symmetric groups S_n, the reader can refer to ref. 41.

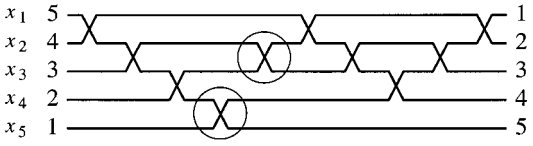

Fig. 13. A diagram associated with a sorting algorithm acting on five element lists. A line follows a number during the sorting process. Each pair of lines cross, only once. The two circled comparators can be exchanged without changing the corresponding tiling.

Figure 13 illustrates this construction. A continuous line follows a number during the sorting process. For example, the greatest number is on the top at the beginning and in the bottom at the end. Since every number must be compared to every other one, and since there is no redundancy, there are $\binom{n}{2}$ crossings.

We are now able to establish the link between those algorithms and $n \to 2$ tilings, more precisely with their de Bruijn representation. Indeed, the analogy between the diagram of Fig. 13 and a de Bruijn grid with one line per family is straightforward: each continuous line of the diagram represents a de Bruijn line and crosses exactly once every other line.

However, there is a fundamental difference between both systems: different sorting algorithms can represent the same de Bruijn grid since only the crossing topology is meaningful. For example, in Fig. 13, the fourth and the fifth comparator (i.e., refs. 4, 5 and refs. 2, 3) are applied in this order (these comparator are circled in the figure). If they were applied in the reverse ordre, the algorithm would be different whereas the de Bruijn grid would be the same.

Therefore we are led to define equivalence classes of sorting algorithms.[42, 28] We say that two comparators $[i, i+1]$ and $[j, j+1]$ commute if $|i-j|>1$. Two algorithms are equivalent if they differ by a finite number a comparator commutations. These equivalence classes of n-element sorting algorithms are in one-to-one correspondence with n-family grids with one line per family, and therefore with tilings inscribed in polygons of side 1. The number A_n of equivalent classes has been computed by Stanley[39] (see also Edelman and Greene[40]) and is given by Eq. (B.1) in the case where $k_i = 1$ for all i:

$$A_n(1, 1, \ldots, 1) = \frac{\binom{n}{2}!}{1^{n-1}3^{n-2}\cdots(2n-3)^1} \tag{B.2}$$

We need to generalize this point of view to systems with more than one line per de Bruijn family, which leads to the definition of *partial* sorting algorithms. These algorithms are related to pre-sorted lists of numbers.

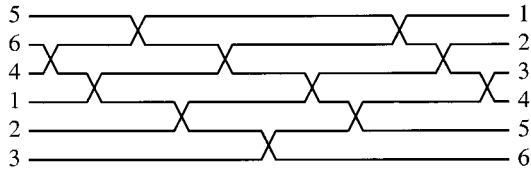

Fig. 14. A partial sorting algorithm in the case of $n=3$ families, containing respectively $k_1=3$, $k_2=1$ and $k_3=2$ pre-sorted elements. The sequence w_0 appears vertically on the left of the figure.

Indeed, let us suppose that we have n families of k_i numbers each ($i=1,...,n$), and that in each family, the numbers are already pre-sorted in the increasing order. Then we are interested in the algorithms which order the whole set of these numbers in the increasing order. We call them partial sorting algorithms. The ideas are essentially the same as in the previous case, except that, since the numbers of a given family are already ordered, the corresponding lines do not need to cross. The corresponding diagram is similar to a de Bruijn grid with n families of lines, k_i lines in each family. The tilings are equivalence classes of such algorithms. They are inscribed in polygons of sides $k_1,..., k_n$.

In the partial sorting case, the reference list to be reversed is not $(n, n-1,..., 1)$ any longer but a list w_0 were some elements are already sorted. If $\kappa_i = k_1 + k_2 + \cdots + k_i$, then

$$w_0 = (\kappa_{n-1}+1,..., \kappa_{n-1}+k_n, \kappa_{n-2}+1,..., \kappa_{n-2}+k_{n-1},..., 1, 2,..., k_1) \qquad \text{(B.3)}$$

There are n pre-sorted blocks of k_i elements each. An example is provided in Fig. 14.

Note also that a sorting algorithm can be seen as an ordering (or a labeling) of the comparators of the corresponding equivalence class, since the comparators come in a natural order: the labels are increasing on each de Bruijn line, from left to right. As a consequence, sorting algorithms are in one-to-one correspondence with labeling of tilings, as defined in Section 3.2 or Appendix A. This point is striking when comparing Figs. 12 and 14. Therefore the sums of the coefficients a_j of a $D \to 2$ problem is equal to the number of partial sorting algorithms of the suitable pre-sorted $D-1$ families of variables. This point will be helpful in the following section.

Appendix B.2. Walks and Symmetric Groups S_n (Algebraic Proof)

The main result used in this section is a theorem by Stanley (Theorem 4.1 of ref. 39, and its Corollary 4.2). We first need to expose

these results and to translate them in terms of our notations and definitions. It is the object of the first paragraph. Then, using the above equivalence between coefficients a_j and partial sorts, we shall apply Stanley's theorem to the case of interest here, and derive relation B.1.

Appendix B.2.1. Stanley's Theorem

The symmetric group S_n of permutations on n elements is generated by the transpositions $\sigma_i = (i, i+1)$: any permutation w can be decomposed in products of transpositions. A decomposition is said to be *minimal* if, using the relations between the generators σ_i:

$$\sigma_i^2 = 1 \qquad \text{and} \qquad \sigma_i \sigma_{i+1} \sigma_i = \sigma_{i+1} \sigma_i \sigma_{i+1} \tag{B.4}$$

it cannot be simplified into a shortest decomposition; then all the reduced decomposition of w have the same length,[13] denoted by $l(w)$. If $w = \left(\begin{smallmatrix} 1 & 2 & \cdots & n \\ a_1 & a_2 & \cdots & a_n \end{smallmatrix}\right)$, we define

$$r_i(w) = \mathrm{Card}\{ j : j < i \text{ and } a_j > a_i \} \tag{B.5}$$

$$s_i(w) = \mathrm{Card}\{ j : j > i \text{ and } a_j < a_i \} \tag{B.6}$$

Then $\lambda(w)$ is the sequence obtained by arranging the numbers $r_i(w)$ in descending order (and ignoring any 0's); $\mu(w)$ is the *conjugate*[14] to the sequence obtained by arranging the numbers $s_i(w)$ in descending order.

Stanley[39] states that: *if $\lambda(w) = \mu(w)$, then the number of reduced decompositions of w is equal to the number $f^{\lambda(w)}$ of standard Young tableaux of shape $\lambda(w)$.*

Appendix B.2.2. Application to Walks in $n \to 1$ Configuration Spaces

We still denote by w_0 the permutation as defined in the previous section. The idea is to see each comparator $[i, i+1]$ as a generator $\sigma_i = (i, i+1)$ of a reduced decomposition and to identify a sorting algorithm with a reduced decomposition of w_0. More precisely, the set of comparators can be seen as the generators of a group, and they obey the same relations as the σ_i: they satisfy relations B.4, and $[i, i+1]$ and $[j, j+1]$ commute if $|i-j| > 1$. Finally, the non-redundant character of sorts is equivalent to the reduced character of decompositions. As a consequence, the number $A_n(k_1, \ldots, k_n)$ of partial sorts is equal to the number of reduced decompositions of w_0.

[13] The length of a decomposition is the number of generators necessary to write it.

[14] If a decreasing sequence is drawn like a Young tableau, its conjugate is the decreasing sequence of row lengths. For example, the conjugate to (3, 2, 2, 1) is (4, 3, 1).

Now, in order to apply Stanley's statement, we must compute the quantities $\lambda(w_0)$ and $\mu(w_0)$, as defined in ref. 39: in the present case, one gets

$$r_i(w_0) = k_n + \cdots + k_j \qquad \text{if} \quad k_n + \cdots + k_j + 1 \geqslant i \geqslant k_n + \cdots + k_{j-1} \tag{B.7}$$

$$s_i(w_0) = \kappa_{j-1} \qquad \text{if} \quad k_n + \cdots + k_j + 1 \geqslant i \geqslant k_n + \cdots + k_{j-1} \tag{B.8}$$

Thus

$$\lambda(w_0) = \mu(w_0) = (\underbrace{k_n + \cdots + k_2}_{k_1 \text{ times}}, \underbrace{k_n + \cdots + k_3}_{k_2 \text{ times}}, \ldots, \underbrace{k_n}_{k_{n-1} \text{ times}}) \tag{B.9}$$

and Stanley's theorem applies. The Young tableau of shape $\lambda(w_0)$ is represented in Fig. 15. Such a tableau will be called a *block tableau* of size $(k_1, k_2, \ldots, k_n)$ in the following. The number $A_n(k_1, k_2, \ldots, k_n)$ of reduced decompositions of w_0 is equal to the number $f^{\lambda(w_0)}$ of standard Young tableaux of shape $\lambda(w_0)$. This number can be derived from Young's *hook-length formula*:[43, 44] given a shape λ, the *hook* associated with a given cell c of the tableau is the set of cells above and at the right of c, including c itself (Fig. 16). It is denoted by H_c. The *hook length* h_c is the number of cells in H_c. Then the number f^λ of standard Young tableaux of shape λ is:

$$f^\lambda = \frac{N!}{\prod_c h_c} \tag{B.10}$$

where N is the total number of cells and the product runs over all cells.

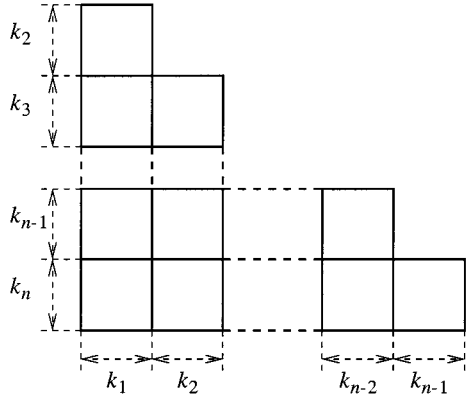

Fig. 15. A Young tableau of shape $\lambda(w_0) = \mu(w_0)$. The numbers k_i denote the number of rows and columns in each rectangular block. Such a tableau is called a block tableau of size $(k_1, k_2, \ldots, k_n)$.

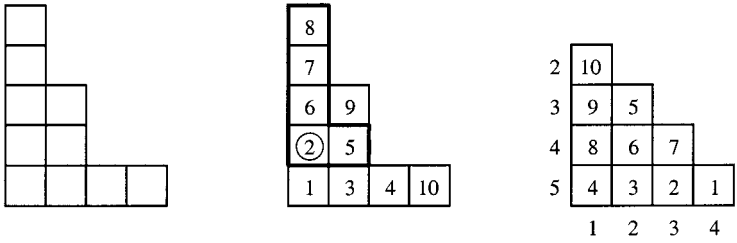

Fig. 16. Left: a four-column Young tableau of shape $\lambda = (5, 3, 1, 1)$. Middle: an associated standard tableau. The hook corresponding to the circled entry is represented. Its length is $h_c = 5$. The hook rank of this cell is $r_c = 1$ and its hook height is $\theta_c = 4$: this tableau is *not* balanced. Right: a balanced stair tableau of order 5.

This hook-length formula can know be applied to the above tableau: the hook-length of the cell in the upper right corner of block $k_i \times k_j$ is $K_{ij} + 1$, from which one deduces all the hook-lengths on the block and their product:

$$\frac{(K_{ij} + k_i + k_j - 1)!^{[2]}\,(K_{ij} - 1)!^{[2]}}{(K_{ij} + k_i - 1)!^{[2]}\,(K_{ij} + k_j - 1)!^{[2]}}$$

Moreover, $N = \sum_{i<j} k_i k_j$, from which Eq. (B.1) follows.

Appendix B.3. Combinatorial Proof

In this section, we provide a combinatorial bijective proof of the previous result.[21] This proof follows the same scheme as the proof by Edelman and Greene[40] in the case where all the parameters k_i are equal to 1. We need first to introduce the notion of *balanced tableaux*.[40]

We consider a Young tableau, together with a labeling of its cells, running from 1 to the number of cells, K. Note that now this tableau is not necessarily standard, that is to say the labels are not necessarily ordered in each row and in each column. Given a cell c and its hook H_c, we define the *hook rank* r_c of c as the number of cells of H_c whose labels are smaller or equal to the label of c. We also define the *hook height* θ_i as the number of cells above c (including c itself). The tableau is said to be balanced if for all cells c, $r_c = \theta_c$ (see Fig. 16).

At last, a tableau of shape $(n-1, n-2, \ldots, 1)$ (Fig. 16, right) will be called a *stair tableau* (of order n). Note that a stair tableau is a particular case of block tableau, as defined in the previous section.

In the case $k_i = 1$, the situation is as follows: Edelman and Greene build a bijection between *complete* sorting algorithms on n elements and balanced block tableaux of order n and then a bijection between those

balanced tableaux and standard tableaux of order n, which are then enumerated *via* the hook-length formula. In the following, we use and generalize these results to the case of partial sorts. In fact, in ref. 40, the authors also establish the bijection between balanced tableaux of any shape and standard tableaux of the same shape. As a consequence, we only need to generalize the first bijection between *partial* sorting algorithms on n families containing k_i elements each and balanced block tableaux of size $(k_1,..., k_n)$, as in Fig. 15. Once this correspondence is established, the rest of the proof is based upon the hook-length formula, as in the previous algebraic proof. The rest of the section is devoted to this correspondence.

To begin with, let us consider a *complete* sorting algorithm on n lines: it is a sequence of crossings between de Bruijn lines. These crossings are labeled by integers running from 1 to $K=\binom{n}{2}$, from left to right. Following Edelman and Greene, the intersection label of two lines indexed by a and b is denoted by t_{ab}. In the stair tableau, this number is written in the cell situated on the ath column and on the $(n-b+1)$th line (starting from the bottom): in Fig. 16 (right), the so-obtained tableau corresponding to the complete sorting algorithm of Fig. 13 is represented. Then it can be proven[40] that this tableau is balanced and more precisely that this construction establishes a bijection between both classes of objects.

Let us now focus on partial sorting algorithms. Since there are couples of de Bruijn lines which do not intersect, it is rather natural to consider block tableaux, which are stair tableaux where some cells are missing. More precisely, we will consider partial sorting algorithms and block

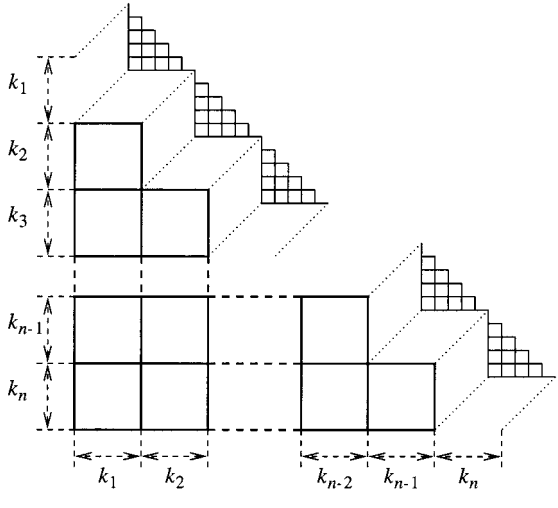

Fig. 17. Amputation of a stair tableau.

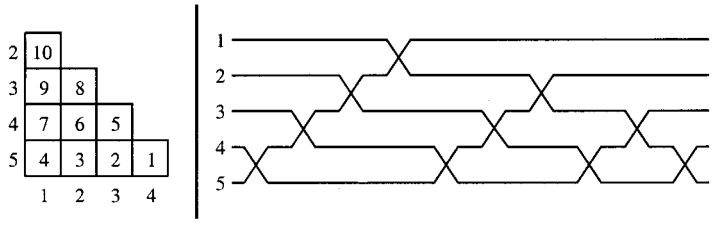

Fig. 18. A canonical complete sort and the corresponding canonical stair tableau.

tableaux as *amputated* complete sorting algorithms and *amputated* stair tableaux, respectively. The idea is to define *canonical* amputations in order to preserve Edelman and Greene's bijection between amputated objects, as discussed below.

Figure 17 illustrates the tableau amputation process: given n integers $k_1,..., k_n$ and a stair tableau of order $N=\sum k_i$, n small stair tableaux of order k_i are removed from the large one in order to get a block tableau of size $(k_1,..., k_n)$.

As far as the amputation of sorting algorithms is concerned, we first need to define *canonical* complete sorts: the simplest way to characterize them is by their corresponding stair tableaux, the cells of which are increasing from left to right and from bottom to top, as illustrated in Fig. 18. They are usually referred as "bubble-sorts" in the literature.

If we consider now a partial sorting algorithm with k_i elements in each family, it can be canonically transformed into a complete sort: we simply add n canonical complete sorts on k_i elements at its end, as in Fig. 19. These sorts appear in the order of their indices i. The so-obtained sort is very particular since it ends with n canonical sorts. Therefore it will be called a *sequential* complete sort of order $(k_1,..., k_n)$. By construction, there is a one-to-one correspondence between sequential complete sorts of order $(k_1,..., k_n)$ and partial sorts of the same size.

Let us now characterize the structure of the Young tableau τ associated with such a sequential sort. The $\binom{k_1}{2}+\binom{k_2}{2}+\cdots+\binom{k_n}{2}$ last intersections in

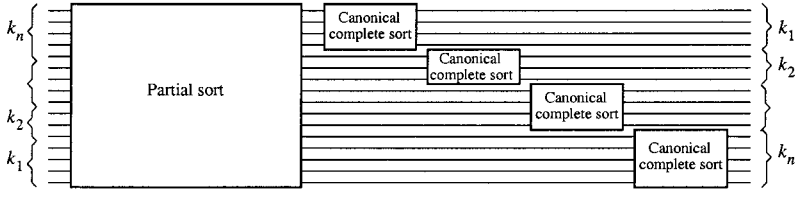

Fig. 19. A complete sequential sorting algorithm: it is a partial sorting algorithm followed by n canonical complete sorts on k_i elements.

the sort are those appearing in the n canonical complete sorts. It is easily checked that the corresponding labels in the large stair tableau appear in the n small canonical stair tableaux involved in the amputation process. As a consequence, the labels of the amputated tableau run from 1 to K, where K is its number of cells. These labels code the K intersections of the partial sort remaining of the original sequential complete sorting algorithm.

To sum up, as it is illustrated in Fig. 20 starting from partial sorts, we biunivocally construct complete sequential sorts, then balanced tableaux, the K last labels of which are situated in the n stair sub-tableaux. When these sub-tableaux are removed from the large one, we obtain a class of block tableaux of size $(k_1,..., k_n)$, which will be called *pre-balanced* tableaux. Remember now that are goal is to establish a bijection between partial sorts and balanced block tableaux. Thus we need to construct a bijection (denoted by R in Fig. 20) between those pre-balanced tableaux of size $(k_1,..., k_n)$ and balanced block tableaux of the same size.

Bijection R. Actually, R is an involution: in each group of k_i columns, it inverses the order of columns; for example, the first column becomes the k_1th one, the second one becomes the (k_1-1)th one and so on. Likewise, the (k_1+1)th column becomes the (k_2-1)th one. There is a rather deep reason for such a column permutation: the n canonical complete

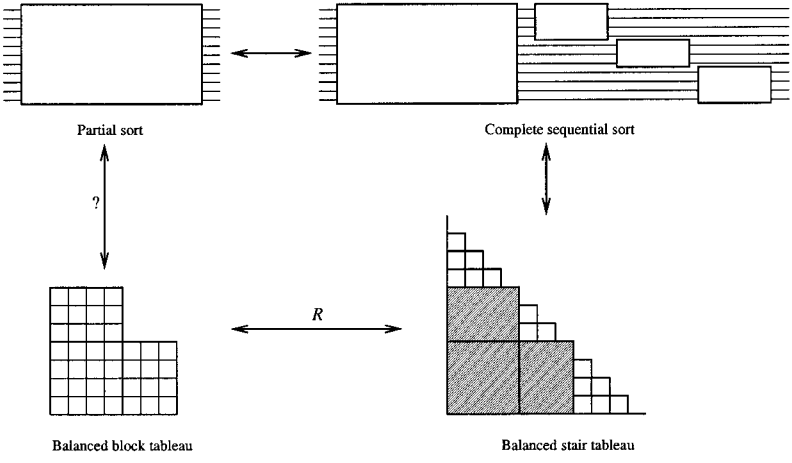

Fig. 20. Sequence of bijections establishing the one-to-one correspondence between partial sorting algorithms on n families with k_i numbers each and balanced block tableaux of size $(k_1,..., k_n)$. In the lower right stair tableau, the grayed sub-tableau is a pre-balanced block one. The bijection R puts such tableaux in one-to-one correspondence with balanced block tableaux of the same shape.

sorts added at the end of a partial sort in order to make it complete also reverse the order of lines in each group of k_i lines. The role of R is to keep track of this fact. It is now a rather technical task to prove that R provides balanced tableaux and that it is a bijective map.

We shall temporarily admit the following results which will be proven at the end of this section: in a pre-balanced tableau, in each block $k_i \times k_j$, the labels are decreasing in each line and column (from bottom to top); in a balanced block tableau, they are increasing in lines and decreasing in columns in such a block.

Consider a pre-balanced block tableau and in this tableau a hook H_c associated with the cell c situated in the block $k_i \times k_j$, and in this block in the line u (from bottom to top) and column v ($1 \leqslant u \leqslant k_i$ and $1 \leqslant v \leqslant k_j$). This hook comes from a larger one, H'_c, in the stair tableau which has been amputated. In the process the hook has lost C cells, C_1 on its right and C_2 on its top (see Fig. 21). Thus the height of H_c is equal to

$$\theta_c = \theta'_c - C_2$$

On the other hand, all the lost cells, coming from the n removed stair tableaux, had labels larger than the label of the cell c. As a consequence, the hook rank remains unchanged:

$$r_c = r'_c$$

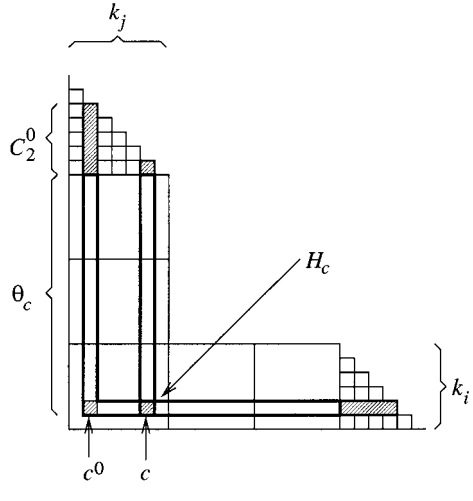

Fig. 21. A hook H_c of a pre-balanced tableau. As compared to the original hook H'_c (before the amputation), it has lost cells on its top and on its right (dashed). By the involution R, c receives the label of the cell c^0.

Now, R permutes the labels of the block tableau but does not change its shape. In the process, the cell c receives the label of the cell c^0 still situated in the line u, but in the column $k_j - v + 1$.

For a given quantity A assigned to each cell, we denote by A^0 the value of this quantity for the cell c^0 in the pre-balanced tableau, and A^R its value in its image by R. In particular, $\theta_c^R = \theta_c^0$, and we have just proven that $r_c^0 - \theta_c^0 = C_2^0$. Moreover, $r_c^R = r_c^0 - (k_j - v^0)$. Indeed, by R, the hook H_c receives the labels of the hook H_{c_0} outside the block $k_i \times k_j$; and in the block, the labels, which were decreasing in the line u of the pre-balanced tableau, are increasing in its image by R. As a consequence,

$$r_c^R - \theta_c^R = C_2^0 - (k_j - v^0)$$

Now $C_2^0 = (k_j - v^0)$ by definition. Therefore $r_c^R = \theta_c^R$ and the tableau is balanced. Conversely, given a balanced tableau, since the labels are increasing in each line of each block, one proves that its image by the involution R is pre-balanced. We have established the bijection.

We need to prove the two above assertions about the order of labels in blocks of balanced and pre-balanced tableaux. We only give sketches of the proofs. As far as pre-balanced tableaux are concerned, the proof is rather straightforward: a block $k_i \times k_j$ contains labels associated with all the intersections of two families of lines. If those lines are isolated from the rest of the tiling, it becomes clear that the order in which intersections occur is constrained. For balanced tableau, the proof is more complex. The basic idea is to construct a proof by "planar induction:" we prove that if a suitable $\mathscr{P}$ property is true for cells above and at the right of a given cell c, then it is also true for c. Then if $\mathscr{P}$ is true for cells on the upper right corners of the tableau, it will be true for every cell. In the present case, if t_c still denotes the label of the cell c, then the property reads:

$\mathscr{P}(c)$: *in the block $k_i \times k_j$ to which c belongs, the cells above c have labels smaller than t_c, while the cells at its right have labels greater than t_c.*

A proper use of the balanced character of a block tableau proves that it satisfies the above planar induction principle.

APPENDIX C. PROOFS OF SECTION 4

In this appendix, we only give sketches of proofs for the results used in Section 4. The complete proofs can be found in the relevant references.

Appendix C.1. Elnitsky's Formulas

In order to prove relations 6 and 7, we need, in the octagonal case, a slightly different representation of de Bruijn grids than those presented in

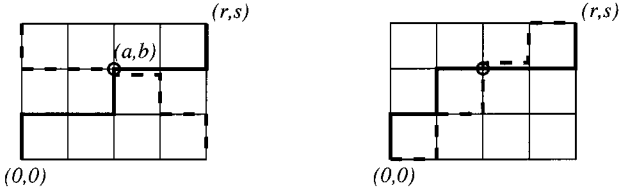

Fig. 22. Two lattice-path diagrams, associated with the two tilings of Fig. 11. The de Bruijn lines of the two single-line families are represented by a pair of paths running on a square lattice. These paths go from one corner to the diagonally opposite one. In case of ambiguity, the vertex where the de Bruijn lines intersect is distinguished by a circle. There are two cases: either the two sides of length one of the polygonal boundary are consecutive (right) or not (left).

the introductory section: as displayed in Fig. 22, the lines of the two first families form a square lattice (of sides r and s in this case), on which the lines of the third and fourth de Bruijn families run: they are represented by directed walks on the lattice, going from one corner to the diagonally opposite one. According to whether the two sides of length one are adjacent or not, the two paths have the same starting and ending points (right) or not (left). In this representation, the de Bruijn line intersections must be distinguished to avoid possible ambiguities due to path tangency (it will be called the *distinguished* vertex in the following). For example, the octagonal tilings of Fig. 11 are represented by the pair of paths of Fig. 22.

The proof of relation 6 is now straightforward: if (a, b) are the coordinates of the distinguished vertex in the grid, then the number of configurations is the product of the 4 number of choices for the four pieces of paths going from (a, b) to the four corners, that is the product of four binomial coefficients. Now summing over all (a, b) configurations one gets relation 6.

The proof of relation 7 is a little more complex and involves some modifications of the pair of paths, as usual in this kind of calculation. The idea is to exchange the two paths *after* the distinguished vertex, in order to get non-crossing (but possibly touching) paths, and then to shift some parts of those paths in order to get a non-touching pair. The latter pairs can be counted with help of the determinental Gessel–Viennot method.[45] The interested reader will refer to ref. 28 for more details.

Appendix C.2. Brock's Recursion Relation

Let us now focus on the recursion relation 10. We use again the lattice-path representation, as defined in the previous section. Given a pair p of crossing paths, with no *a priori* distinguished vertex, let us denote by l_p the length of their intersection (see Fig. 23). Note that this intersection can

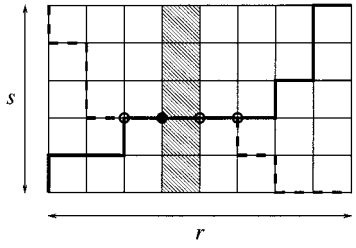

Fig. 23. When the two path intersection is a segment (vertical or horizontal, of length $l_p > 0$; here $l_p = 3$), the same pair can represent several tilings, depending on the position of the distinguished vertex. If this point is not the last possible one (i.e., the point with the highest coordinates), then a strip of the lattice can be removed (dashed in this figure, at the right of the black distinguished vertex). The so-obtained diagram is associated with a smaller tiling ($r-1 \times s$ in the present case; $r \times s-1$ if the segment were vertical).

be a point ($l_p = 0$), a horizontal or a vertical segment (of length l_p). If $\mathscr{P}_{r,s}$ is the set of pairs, then

$$W^{4\to 2}_{r,1,s,1} = \sum_{p\in\mathscr{P}_{r,s}} l_p + 1 = \binom{r+s}{r}^2 + \sum_{p\in\mathscr{P}_{r,s}} l_p \tag{C.1}$$

since there are $l_p + 1$ possible choices for the distinguished vertex and there are $\binom{r+s}{r}^2$ such pairs of paths.

In the case where $l_p > 0$, if the distinguished vertex is not the point with the highest coordinates (l_p possibilities), as in Fig. 23, then a vertical or horizontal strip of the square lattice can be removed without changing the nature of the diagram: it is the strip of width 1, at the right of (respectively above) the distinguished vertex if the intersection is horizontal (respectively vertical). As a result, one still have a square lattice (but one of its side lengths is lowered by 1) with a pair of paths (but the length of their intersection has been lowered by one in the process). That is why

$$\sum_{p\in\mathscr{P}_{r,s}} l_p = \sum_{p\in\mathscr{P}_{r-1,s}} (l_p+1) + \sum_{p\in\mathscr{P}_{r,s-1}} (l_p+1) \tag{C.2}$$

In conclusion,

$$\begin{aligned} W^{4\to 2}_{r,1,s,1} &= \binom{r+s}{r}^2 + \sum_{p\in\mathscr{P}_{r,s}} l_p \\ &= \binom{r+s}{r}^2 + \sum_{p\in\mathscr{P}_{r-1,s}} (l_p+1) + \sum_{p\in\mathscr{P}_{r,s-1}} (l_p+1) \\ &= \binom{r+s}{r}^2 + W^{4\to 2}_{r-1,1,s,1} + W^{4\to 2}_{r,1,s-1,1} \end{aligned} \tag{C.3}$$

which achieves the proof.

APPENDIX D. WHAT ABOUT THE GENERAL $D \to d$ CASE?

In this last appendix, we discuss what we know and what we do not know about the general $D \to d$ case which was more widely studied in ref. 21. The different points and results tackled in the present paper are discussed. It will become clear that the possible existence of cycles in the partition-on-tiling problems is the major obstacle to simple generalizations.

Appendix D.1. Partition-on-Tiling Point of View and Configuration Space

As far as partitions on tilings are concerned, all that as been said in the octagonal case can be transposed to the general case: a fixed boundary $D \to d$ tiling[3, 21] can be coded in a single way as a partition on a $D-1 \to d$ tiling. The de Bruijn lines are still defined as lines joining together the middles of opposite faces of rhombic tiles, and the parts of those partitions are still increasing along such lines. The reader can refer to Bailey[23] for a more formal treatment of this question. Note that in this case, there also exist de Bruijn families of *hyper-surfaces*, associated with an edge orientation.

However, as it was suggested in ref. 3, the geometry of configuration spaces might be more complex beyond the octagonal case. Indeed, among the order relations $x_i \geqslant x_j$ between the parts of a partition-on-tiling problem, nothing forbids *a priori* the existence of cycles of inequalities, such as $x_{i_1} \geqslant x_{i_2} \geqslant \cdots \geqslant x_{i_q} \geqslant x_{i_1}$, which enforces all these variables to be equal.

At least two examples of $6 \to 3$ tilings (in relation with $7 \to 3$ tiling problems) are known which display such cycles. The first one can be found in ref. 46 (Example 10.4.1) and the second one in ref. 47 (Example 3.5).[15] In these examples, the tilings are defined by their dual de Bruijn grids—which are families of 2-dimensional de Bruijn surfaces in a 3-dimensional space—together with an orientation of de Bruijn lines.

When such a cycle exists, all the parts of the cycle have a "collective behavior," which is not compatible with the previous description: they behave like a single *effective* part. In particular, the number of effective parts in this partition problem, denoted as K', is strictly smaller than K. Thus the counting polynomial of this partition problem becomes:

$$\sum_{j=0}^{M'} a_j^{K'} \binom{K'+p-j}{K'} \tag{D.1}$$

[15] Note that in these references (Proposition 10.5.7 of ref. 46 and Corollary 4.5 of ref. 47), it is also stated that no such cycles exist in two-dimensional tilings.

The counting polynomial of the whole tiling problem is a sum of such polynomials, with possibly many different K'.

Moreover, the existence of cycles invalidates the proof of the connectivity of the configuration space (Section 2.2). As far as we know, this point is an open question in the general $D \to d$ case. Note however that whenever one can prove that order relations on fibers contain no cycles, then the configuration space is connected.

Appendix D.2. Decomposition in Simplices—Descent Theorem

We prove that the existence of cycles does not alter the previous results about the sums of coefficients a_j and walks in configuration spaces, provided these objects are suitably defined: if we focus only on coefficients a_j^K associated with configuration spaces of effective dimension K (and not $K' < K$), then the sum $\sum^K$ of these coefficients is equal to the number of maximal walks in the corresponding $D-1 \to d-1$ configuration space. Note that this quantity $\sum^K$ still characterizes the leading coefficient of the counting polynomial (of degree K) as p goes to infinity.

More precisely, if there exists a cycle in the partition problem on a membrane, we have just seen that the coefficients $a_j^{K'}$ of this problem do not contribute to $\sum^K$. On the other hand, let us consider a step in a walk in the $D-1 \to d-1$ configuration space: we have seen that the part x which differentiates the two consecutive configurations of this step is such that all parts lesser (resp. greater) than x in the graph are equal to 1 (resp. 0). This part is equal to 0 in a partition and to 1 in the other one. As far as the parts of the cycle are concerned, since they are all equal, they cannot but jump from 0 to 1 all together, which is not conform to our definition of walk in the configuration space, in terms of *single* elementary flips. Conversely and for similar reasons, a maximal walk in the configuration space cannot give a membrane with cycles.

In conclusion, as well $\sum^K$ as the number of walks are not concerned by partitions with cycles, and the above result remains valid.

Before going on, let us specify what the extremal tilings become in larger dimension: $C_{\min}$ and $C_{\max}$ are defined by partitions where all the parts are equal to 0 and 1, respectively. Therefore the corresponding tilings present a faceted aspect, as on Fig. 24. Note that among the different possible faceted tilings, the two extremal ones depend on how the Dth de Bruijn family of surfaces is chosen.

At last, we recall that there cannot exist a descent theorem as simple as the octagonal one in the general case. Indeed, its derivation is closely related to the existence of a zero-descent simplex in each partition-on-tiling

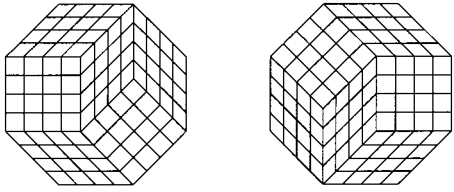

Fig. 24. Two examples of extremal $4 \to 2$ tilings displaying a macroscopic faceting. Such tilings are extremal configurations for walks associated with a $5 \to 3$ problem. There are four similar pairs of faceted tilings which could be chosen as extremal configurations, depending on how the fourth de Bruijn family is chosen among the four possible ones.

problem, that is to the K-dimensional character of the associated configuration space. But we have shown that this point is not granted in general, since there can exist partition-on-tiling problems for which the configuration space has a dimension K' smaller than K.

ACKNOWLEDGMENTS

We wish to express our gratitude to Mike Widom, Matthieu Latapy and Vic Reiner for fruitful discussions and helpful comments.

REFERENCES

1. D. Shechtman, I. Blech, D. Gratias, and J. W. Cahn, Metallic phase with long-range orientational order and no translational symmetry, *Phys. Rev. Lett.* **53**:1951 (1984).
2. R. Penrose, The role of aesthetics in pure and applied mathematical research, *Bull. Inst. Math. Appl.* **10**:226 (1974).
3. N. Destainville, R. Mosseri, and F. Bailly, Configurational entropy of codimension-one tilings and directed membranes, *J. Stat. Phys.* **87**(3/4):697 (1997).
4. N. Wang, H. Chen, and K. H. Kuo, Two-dimensional quasicrystal with eightfold rotational symmetry, *Phys. Rev. Lett.* **59**:1010 (1987).
5. W. Li, H. Park, and M. Widom, Phase diagram of a random tiling quasicrystal, *J. Stat. Phys.* **66**(1/2):1 (1992).
6. M. Widom, Bethe ansatz solution of the square–triangle random tiling model, *Phys. Rev. Lett.* **70**:2094 (1993).
7. P. A. Kalugin, The square–triangle random-tiling model in the thermodynamic limit, *J. Phys. A: Math. Gen.* **27**:3599 (1994).
8. J. de Gier and B. Nienhuis, Exact solution of an octagonal random tiling model, *Phys. Rev. Lett.* **76**:2918 (1996).
9. J. de Gier and B. Nienhuis, Bethe ansatz solution of a decagonal rectangle–triangle random tiling, *J. Phys. A: Math. Gen.* **31**:2141 (1998).
10. M. Widom, N. Destainville, R. Mosseri, and F. Bailly, Two-dimensional random tilings of large codimension, in *Proceedings of the 6th International Conference on Quasicrystals* (World Scientific, 1998).

11. R. Mosseri and F. Bailly, Configurational entropy in octagonal tiling models, *Int. J. Mod. Phys. B* **7**(6/7):1427 (1993).
12. V. Elser, Comment on "Quasicrystals: a new class of ordered structures," *Phys. Rev. Lett.* **54**:1730 (1985).
13. M. Duneau and A. Katz, Quasiperiodic patterns, *Phys. Rev. Lett.* **54**:2688 (1985).
14. A. P. Kalugin, A. Y. Kitaev, and L. S. Levitov, $Al_{0.86}Mn_{0.14}$: A six-dimensional crystal, *JETP Lett.* **41**:145 (1985); A. P. Kalugin, A. Y. Kitaev, and L. S. Levitov, 6-dimensional properties of $Al_{0.86}Mn_{0.14}$, *J. Phys. Lett. France* **46**:L601 (1985).
15. N. G. de Bruijn, Algebraic theory of Penrose's non-periodic tilings of the plane, *Kon. Nederl. Akad. Wetensch. Proc. Ser. A* **43**:84 (1981).
16. N. G. de Bruijn, Dualization of multigrids, *J. Phys. France* **47**:C3–9 (1986).
17. J. E. S. Socolar, P. J. Steinhardt, and D. Levine, Quasicrystals with arbitrary orientational symmetry, *Phys. Rev. B* **32**(8):5547 (1985).
18. F. Gähler and J. Rhyner, Equivalence of the generalized grid and projection methods for the construction of quasiperiodic tilings, *J. Phys. A: Math. Gen.* **19**:267 (1986).
19. V. Elser, Solution of the dimer problem on an hexagonal lattice with boundary, *J. Phys. A*: *Math. Gen.* **17**:1509 (1984).
20. R. Mosseri, F. Bailly, and C. Sire, Configurational entropy in random tiling models, *J. Non-Cryst. Solids* **153**–**154**:201 (1993).
21. N. Destainville, Ph.D. Thesis: "Entropie configurationnelle des pavages aléatoires et des membranes dirigées," Thèse de l'Université Paris 6 (1997).
22. N. Destainville, Entropy and boundary conditions in random rhombus tilings, *J. Phys. A: Math. Gen.* **31**:6123 (1998).
23. G. D. Bailey, *Tilings of Zonotopes: Discriminental Arrangements*, *Oriented Matroids and Enumeration* (Minnesota University Thesis, 1997).
24. H. Cohn, M. Larsen, and J. Propp, The shape of a typical boxed plane partition, *New York J. of Math.* **4**:137 (1998).
25. H. Cohn, R. Kenyon, and J. Propp, A variational principle for domino tilings, *J. of AMS*. (to appear).
26. M. Latapy, Generalized integer partitions, tilings of zonotopes and lattices, preprint.
27. R. Kenyon, Tilings of polygons with parallelograms, *Algorithmica* **9**, 382 (1993).
28. S. Elnitsky, Rhombic tilings of polygons and classes of reduced words in Coxeter groups, *J. Combinatorial Theory A* **77**:193 (1997).
29. R. P. Stanley, Ordered structures and partitions, *Memoirs of the AMS* **119** (1972).
30. V. Strehl, Combinatorics of special functions: facets of Brock's identity, in *Séries Formelles et Combinatoire Algébrique*, P. Leroux and C. Reutanauer, eds. (University of Québec, Montreal, 1992).
31. C. L. Henley, Relaxation time for a dimer covering with height representation, *J. Stat. Phys.* **89**:483 (1997).
32. D. Randall and P. Tetali, Analyzing Glauber dynamics by comparison of Markov chains, in *Proceedings of the 3rd Latin American Theoretical Informatics Symposium*, Springer Lecture Notes in Computer Science, Vol. 1380, p. 292 (1998).
33. M. Luby, D. Randall, and A. Sinclair, Markov chain algorithms for planar lattice structures, preprint.
34. D. B. Wilson, Mixing times of lozenge tiling and card shuffling Markov chains, preprint.
35. R. Mosseri and J.-F. Sadoc, Glass-like properties in quasicrystals, in *Proceedings of the 5th International Conference on Quasicrystals*, C. Janot and R. Mosseri, eds. (World Scientific, 1995), p. 747.
36. L. Leuzzi and G. Parisi, *A Tiling Model for Glassy Systems*, preprint (cond-mat/9911020).

37. K. J. Strandburg and P. R. Dressel, Thermodynamic behavior of a Penrose-tiling quasicrystal, *Phys. Rev. B* **41**:2469 (1990).
38. Y. Ishii, Dynamics of phason relaxation on Penrose lattices, in *Proceedings of the 5th International Conference on Quasicrystals*, C. Janot and R. Mosseri, eds. (World Scientific, 1995), p. 359.
39. R. P. Stanley, On the number of reduced decompositions of elements of Coxeter groups, *European J. of Comb.* **5**:359 (1984).
40. P. Edelman and C. Greene, Balanced tableaux, *Adv. in Math.* **63**:42 (1987).
41. B. E. Sagan, *The Symmetric Group* (Wadsworth and Brooks, California, 1991).
42. D. M. Knuth, Axioms and hulls, *Lect. Notes in Computer Sci.* **606**:35 (1992).
43. A. Young, On quantitative substitutional analysis, *Proc. London Math. Soc. 2* **28**:255 (1927).
44. C. Greene, A. Nijenhuis, and H. S. Wilf, A probabilistic proof of a formula for the number of Young tableaux of a given shape, *Adv. in Math.* **31**:104 (1979).
45. I. Gessel and G. Viennot, Binomial determinants, paths and hook lenght formulae, *Adv. in Math.* **58**:300 (1985).
46. A. Björner, M. Las Vergnas, B. Sturmfels, N. White, and G. M. Ziegler, *Oriented Matroids* (Cambridge University Press, 1993).
47. B. Sturmfels and G. M. Ziegler, Extention spaces of oriented matroids, *Discrete & Computational Geom.* **10**:23 (1993).